Journal of Statistical Software

October 2025, Volume 114, Issue 12. *doi: 10.18637/jss.v114.i12*

Benchpress: A Versatile Platform for Structure Learning in Causal and Probabilistic Graphical Models

Felix L. Rios
University of Basel

Giusi Moffa
University of Basel

Jack Kuipers
ETH Zürich

Abstract

Describing the relationship between the variables in a study domain and modeling the data generating mechanism is a fundamental problem in many empirical sciences. Probabilistic graphical models are one common approach to tackle the problem. Learning the graphical structure for such models is computationally challenging and a fervent area of current research with a plethora of algorithms being developed. To facilitate the benchmarking of different methods, we present a novel **Snakemake** workflow, called **Benchpress** for producing scalable, reproducible, and platform-independent benchmarks of structure learning algorithms for probabilistic graphical models. **Benchpress** is interfaced via a simple JSON-file, which makes it accessible for all users, while the code is designed in a fully modular fashion to enable researchers to contribute additional methodologies. **Benchpress** currently provides an interface to a large number of *state-of-the-art* algorithms from libraries such as **BDgraph**, **BiDAG**, **bnlearn**, **causal-learn**, **gCastle**, **GOBNILP**, **pcalg**, **scikit-learn**, **TETRAD**, and **trilearn** as well as a variety of methods for data generating models and performance evaluation. Alongside user-defined models and randomly generated datasets, the workflow also includes a number of standard datasets and graphical models from the literature, which may be included in a benchmarking study. We demonstrate the applicability of this workflow for learning Bayesian networks in five typical data scenarios. The source code and documentation is publicly available from `https://benchpressdocs.readthedocs.io/`.

Keywords: reproducibility, scalable benchmarking, causal discovery, probabilistic graphical models, structure learning.

1. Introduction

Probabilistic graphical models play a central role in modern statistical data analysis. Their compact and elegant way of visualizing and representing complex dependence structures in multivariate probability distributions has shown to be successfully applicable in many scientific domains, ranging from disciplines such as social sciences and image analysis to biology, medical diagnosis and epidemiology (see, e.g., Elwert 2013; Friedman, Linial, Nachman, and Pe'er 2000; Friedman 2004; Moffa *et al.* 2017; Kuipers *et al.* 2018; Kuipers, Moffa, Kuipers, Freeman, and Bebbington 2019).

One of the main advantages of graphical models is that they provide a tool for experts and researchers from non-statistical fields to easily specify their assumptions in a given problem domain, in a highly transparent way. However, in many realistic situations, the number of variables is either too large to build networks by hand, as it is for example the case in genomic applications, or simply no prior knowledge is available about the relationships between different variables. Consequently, there has been a growing interest in automated strategies to infer the graph component of a probabilistic graphical model from data, so-called *structure learning* or *causal discovery*. For recent reviews of the wide flora of algorithms that have emerged in the last two decades, the reader is referred to Koski and Noble (2012); Kitson, Constantinou, Guo, Liu, and Chobtham (2023).

Since the scientific principle of reproducibility is instrumental for high-quality standards in research, there is an increasing demand to present new algorithms with publicly available source code and datasets (see e.g., Munafò *et al.* 2017; Lamprecht *et al.* 2020). With publicly available software we should, in principle, be able to easily compare different methods with respect to their performance in different settings. The reality is that the practical implementation of new approaches displays high levels of heterogeneity in many aspects, rendering comparative studies challenging and time-consuming. One of the main difficulties is that different algorithms may be implemented in different programming languages, with different dependencies. Different packages may differ with respect to the representation of graphical models, the data formats, and the way they interface to the user, e.g., through the command-line arguments, a configuration file, or a function in a specific programming language. Another complication is that the number of computations increases rapidly in comparison studies, especially when input parameters are altered, which requires parallel computation capabilities and careful bookkeeping to record and organize the results for reporting. As a result, researchers may invest considerable effort in producing benchmarking scripts, and may only be able to implement comprehensive comparisons for a handful of relevant algorithms. To complicate matters further, there is no single well-established metric to evaluate the performance of structure learning algorithms. On the contrary, there is a wide range of different metrics to choose from (see, e.g., Tsamardinos, Brown, and Aliferis 2006; Scutari, Graafland, and Gutiérrez 2019a; Constantinou, Liu, Chobtham, Guo, and Kitson 2021) and researchers tend to evaluate new algorithms on a small subset of selected criteria, typically focusing on those most well suited to the specifics of their method.

When it comes to datasets, there are standard choices commonly used in the literature for benchmarking new algorithms. While desirable to reduce the researchers' degrees of freedom in the choice of data, focusing on a limited set of data examples may have damaging effects by unintentionally leading to solutions artificially tailored to the data properties, rather than agnostically targeting structure learning. Despite the ongoing rapid advances in causal discovery algorithms, unified approaches are still lacking for simulating benchmarking data that display realistic features and are easily accessible to the user. A recent effort to address this need utilizes assembly lines' data for generating semi-synthetic manufacturing data with known causal relationships (Göbler, Windisch, Drton, Pychynski, Roth, and Sonntag

2024). Another line of work focuses on generating data from models violating the standard assumptions for causal discovery (Montagna *et al.* 2023).

With the problems described above in mind, the objective of this work is to develop a unified framework to facilitate the execution and benchmarking of different algorithms. We present a novel **Snakemake** (Köster and Rahmann 2012) workflow called **Benchpress**, which is designed for reproducible, platform-independent, and fully scalable benchmarks of structure learning algorithms. **Benchpress** is interfaced via an easy-to-use configuration file in JSON-format (Pezoa, Reutter, Suarez, Ugarte, and Vrgoč 2016), where a benchmark setup is specified in a module-based *probabilistic programming* style, separating model specification, in terms of graph and corresponding parameters, from algorithm execution and evaluation. **Snakemake** enables **Benchpress** to seamlessly scale the computations to server, cluster, grid and cloud environments, without any changes in the configuration file. The support for containerized software through, e.g., **Apptainer** (Kurtzer, Sochat, and Bauer 2017) or **Docker** (Merkel 2014) images, together with platform-independent representations of data sets and graphs enables **Benchpress** to compare algorithms from different libraries, possibly implemented in different programming languages and with different dependencies. Creating a consensus benchmark setup may mitigate distortions in the performance comparison inadvertently resulting from researchers' degrees of freedom. At the same time, the possibility of easily designing reproducible benchmarking settings will encourage researchers to conduct more comprehensive comparison studies on different datasets and using different metrics.

Benchpress is implemented in a modular coding style with the functionality for researchers to contribute additional modules for generating models, structure learning algorithms and evaluating results. In the current publicly released version we have already included 55 algorithm modules from some of the most popular libraries such as **BDgraph** (Mohammadi and Wit 2019), **BiDAG** (Suter, Kuipers, Moffa, and Beerenwinkel 2023), **bnlearn** (Scutari 2010), **causal-learn** (Zheng *et al.* 2024), **gCastle** (Zhang *et al.* 2021), **GOBNILP** (Cussens 2020), **pcalg** (Kalisch, Mächler, Colombo, Maathuis, and Bühlmann 2012), **r.blip** (Scanagatta, De Campos, Corani, and Zaffalon 2015), **scikit-learn** (Pedregosa *et al.* 2011), **TETRAD** (Glymour and Scheines 1986), and **trilearn** (Olsson, Pavlenko, and Rios 2019) along with models and data sets from the standard literature. See Table 6 in the Appendix for a complete list of the currently available algorithms.

With comparable intent, Constantinou, Liu, Chobtham, Guo, and Kitson (2020) developed **Bayesys**, albeit exclusively designed for *Bayesian networks*, a specific type of probabilistic graphical models (Pearl 1997). Furthermore **Bayesys** is a Java implementation only including six algorithms for structure learning at the time of writing. Another tool called **causal-compare** with a similar purpose to **Benchpress** was released as part of the **TETRAD** project (Ramsey, Malinsky, and Bui 2020). However, the functionality of **causal-compare** is restricted to the algorithm implementations in the **TETRAD** project, representing only a subset of available algorithms from the literature. Overall **Benchpress** offers wider scope and usability than currently available alternatives since **Benchpress** only requires **Docker**, without placing any special requirements on the implementation of individual algorithms.

Benchpress is distributed under the GPL v2.0 License, encouraging its use in both, academic and commercial settings. Source code and documentation are available from `https://benchpressdocs.readthedocs.io/`.

The rest of the paper is structured as follows. Section 2 presents an introduction to graphical models along with some notational conventions. Section 3 provides background on current strategies for structure learning. Section 4 describes the structure of the JSON interface and the modules already available for benchmarking. In Section 5, we show how to use **Benchpress** in several typical benchmarking scenarios. Installation and usage guidelines are provided in Section 6, while Section 7 discusses how to add new algorithms to the **Benchpress** framework.

2. Probabilistic graphical models

This section provides a brief introduction to graphical models and graph theory, with definitions as in, e.g., Diestel (2005); Lauritzen (1996). Let P be a p-dimensional distribution and let $Y := (Y_i)_{i=1}^p$ be a random vector such that $Y \sim \mathsf{P}$. Further let $G = (V, E)$ be a graph, where $V = \{Y_i\}_{i=1}^p$ is the node set and E is the edge set, consisting of ordered pairs of distinct elements of V. Then P, or alternatively Y, is said to be Markov with respect to G if separation, based on some graphical criteria, of two subsets of nodes, Y_A and Y_B, by a third set Y_C in G implies their conditional independence in P, where $Y_A := (Y_i)_{i\in A}$. The term probabilistic graphical model or graphical model has been used interchangeably in the literature to refer to either the tuple (G, P) or a collection of distributions $\mathcal{P}_G$, usually restricted to some specific parametric family, where every $\mathsf{P}' \in \mathcal{P}_G$ is Markov with respect to G. In this text, we will use the former meaning. In the case where P is restricted to a specific parametric family, it is usually uniquely determined by some parameter vector Θ, thus either notation may be used.

Assuming f is a density for P, conditional independence between the random variables Y_A and Y_B given Y_C is well-defined as $f(y_A \mid y_B, y_C) = f(y_A \mid y_C)$, where $\mid y_A, y_B, y_C) \in \mathcal{Y}_A \times \mathcal{Y}_B \times \mathcal{Y}_C$ and $\mathcal{Y}_A$ denotes the range of Y_A. In contrast, node separation may have different definitions depending on the type of graph considered. Typical classes of graphs are: *undirected graphs*, where edges are specified as unordered tuples and separation of Y_A and Y_B given Y_C means that every path between Y_A and Y_B must pass Y_C; *directed acyclic graphs* (DAGs), where edges are represented as ordered tuples and separation is defined by a concept known as *d-separation*, see, e.g., Pearl (1997). Next follows a brief introduction to the type of graphical models currently implemented in **Benchpress**.

Bayesian networks constitute one of the most popular classes of graphical models, referring to distributions that are Markov with respect to a DAG. The conditional independence encoded by the DAG implies that the density can be factorized into local conditional densities, where each node Y_i is directly dependent on its *parents*, $\mathrm{pa}(Y_i)$, as

$$f(y) = \prod_{i=1}^{p} f(y_i \mid \mathrm{pa}(y_i)),$$

where $f(y_i \mid \mathrm{pa}(y_i))$ denotes the conditional density of Y_i given $\mathrm{pa}(Y_i) = \mathrm{pa}(y_i)$. This property is appealing for several reasons. Firstly, the decomposition into local conditional probability distribution provides an intuitive way to express and visualize knowledge about a specific problem domain. In particular, an expert could express a causal mechanism in terms of a DAG, which in turn provides a mathematical language to answer causal queries from non-experimental data (Pearl 1995). Further, it enables fast computations of conditional and marginal distribution using message-passing algorithms by exploiting the factorization property in the distribution. However, when the DAG is not used for expressing causal knowledge, the direction of the edges may be misleading since the conditional independencies of a distribution are not uniquely encoded by a single DAG in general but rather by a class of *Markov equivalent* DAGs, all of which encode the same conditional independence statements. One way to represent a Markov equivalence class is by a *completed partially directed acyclic graph* (CPDAG, see Chickering 1995). A CPDAG is a partially directed DAG which can be obtained from a DAG by regarding an edge (Y_i, Y_j) as undirected if and only if both directed edges (Y_i, Y_j) and (Y_j, Y_i) are present in some of the DAGs in the same equivalence class. The CPDAG is also sometimes called the *essential graph*. An equivalent way to represent the conditional independence statements in a DAG is through the *pattern graph*. The pattern graph of a DAG is the graph obtained by keeping the directions of the *v-structures* and regarding the remaining edges as undirected. v-structures are characterized by triples of nodes where the edges of two of the nodes, which should not be neighbors, are pointing to the third.

Markov networks or *Markov random fields* are another popular class of graphical models, referring to distributions that are Markov with respect to an undirected graph. There is, in general, no decomposition into local densities for the models in this class. However, there exist functions $\{\phi_C\}_{C\in\mathcal{C}}$ such that

$$f(y) = \prod_{C\in\mathcal{C}} \phi_C(y_C),$$

where $\mathcal{C}$ is the set of maximal subgraphs where all nodes are directly connected with each other, usually called *cliques*, which may be leveraged to calculate marginal distributions efficiently. There is a sub-class of undirected graphs called *decomposable* (DG) or *chordal* or *triangulated*, where each cycle with more than three nodes has a *chord*, an edge which breaks it. Distributions which are Markov with respect to decomposable graphs are called *decomposable* and their densities are built by local, clique-specific densities, $\{f_C\}_{C\in\mathcal{C}}$ and their marginals so that the joint density factorizes as

$$f(y) = \frac{\prod_{C\in\mathcal{C}} f_C(y_C)}{\prod_{S\in\mathcal{S}} f_S(y_S)},$$

where $\mathcal{S}$ is the multi-set of separators in G, found, e.g., as the intersection of neighboring cliques in a so-called *junction tree*, built from the cliques in the graph; see, e.g., Lauritzen (1996) for details. In general Markov networks and Bayesian networks encode different sets of conditional independence statements, and there are sets which we can represent with one model but not the other. Decomposable graphs represent the intersection of those sets of statements which we can represent by both undirected graphs and DAGs (see, e.g., Lauritzen 1996; Cowell, Dawid, Lauritzen, and Spiegelhalter 2003; Koller and Friedman 2009). The DAGs representing the intersection set are called *perfect*, meaning that all the parents of each node are connected by an edge. Further characterizations of decomposable graphs are found in, e.g., Lauritzen (1996); Cowell *et al.* (2003) and Duarte and Solus (2023).

3. Structure learning

Structure learning algorithms for Bayesian networks were proved to be NP-hard, even when the number of parents of each node is restricted to two (Chickering, Heckerman, and Meek 2004). Also, the number of undirected graphs grows as $\mathcal{O}(2^{p^2})$ even when restricted to decomposable graphs, making an exhaustive search for a specific graph infeasible (see, e.g., Wormald 1985; Olsson, Pavlenko, and Rios 2022; Hébert-Johnson, Lokshtanov, and Vigoda 2023). Therefore, in practice, we must rely on approximation methods which we can divide into three main categories: *constraint-based*, *score-based*, and *hybrid* algorithms, discussed briefly below.

The seed for the first constraint-based algorithm was planted by Verma and Pearl (1991) in the context of causal Bayesian networks. In line with their work, constraint-based methods employ conditional independence tests among the variables to first estimate an undirected graph by, e.g., starting with the complete graph, and excluding an edge (Y_i, Y_j) if there exists some set Y_A such that the hypothesis $Y_i \perp\!\!\!\perp_{\mathsf{P}} Y_j \mid Y_A$ cannot be rejected according to a suitable test procedure. Such methods tend to be very fast but testing can suffer from large numbers of false negatives, i.e., falsely not including edges when they should be present. Relaxing the significance level of the tests to reduce false negatives can, however, rapidly inflate false positives and runtimes.

Score-based methods on the other hand aim to optimize a global score function defined on the graph space. As a workaround to cope with the immense number of graphs, the search is often limited to certain types of graphs. For example in DAG models, one may restrict the number of parents or combine DAGs into larger and more easily represented classes (e.g., orders and partitions Friedman and Koller 2003; Kuipers and Moffa 2017). For decomposable graphs, a possibility is to limit the maximal clique size. Score functions may rely on penalized log-likelihoods or on Bayesian posterior probabilities of graphical structures conditional on the observed data (see, e.g., Koller and Friedman 2009). Besides mere optimization, Bayesian structure learning also focuses on sampling procedure to provide a finer characterization of the posterior graph distribution. When an expression for the posterior distribution is available at least up to a normalizing constant, we can implement Markov chain Monte Carlo (MCMC) schemes to sample from it, see, e.g., Madigan, York, and Allard (1995); Giudici and Castelo (2003); Friedman and Koller (2003) for early works and Kuipers and Moffa (2017); Jennings and Corcoran (2018) for more recent strategies. In Gaussian Markov networks, Monte Carlo sampling turns out to be infeasible for larger networks since there is in general no analytic expression for the un-normalised posterior (Atay-Kayis and Massam 2005). On the other hand, score-based methods such as *graphical lasso*, rely on the fact that the edges in the graph are revealed from the non-zero pattern of the elements in the precision (inverse covariance) matrix. Optimization techniques can successfully estimate the L_1-penalized log-likelihood of the precision matrix, and the graph as a by-product; see Friedman, Hastie, and Tibshirani (2008); Meinshausen (2008); Witten, Friedman, and Simon (2011). Decomposable models, do possess a closed form expression for the un-normalised graph posterior and most inferential methods built on the representation via undirected graphs focus on Monte Carlo sampling (see, e.g., Giudici and Green 1999; Green and Thomas 2013; Elmasri 2017; Olsson *et al.* 2019) with a few focusing on optimization (see, e.g., Carvalho 2006; Studený and Cussens 2017; Rantanen, Hyttinen, and Järvisalo 2017).

Hybrid algorithms typically use constraint-based algorithms as a preliminary step called *restrict phase* to reduce the search space for a score-based method. A score based-algorithm is then used in the *maximize phase* (see, e.g., Tsamardinos, Aliferis, Statnikov, and Statnikov 2003; Scanagatta *et al.* 2015; Kuipers, Suter, and Moffa 2022).

4. Benchpress modules and JSON configuration files

In this section, we describe the modules of **Benchpress** and the structure of the JSON (Pezoa *et al.* 2016) configuration file, which serves as the interface for the user. As **Benchpress** is implemented as a **Snakemake** workflow, a brief overview of the latter will help to illustrate the overall concept of the tool. **Snakemake** is a highly popular workflow management system with a custom `Python`-based programming language enabling the so-called **Snakemake** *rules*, which build the core of a workflow. Each rule typically comprises four types of fields: the `input` and `output` fields, defining the input and output files, respectively, the `script` and `container` fields, defining the script for generating the output files based on the input files, and the **Docker** image used for running the script, respectively.

When requesting an output file from a specific rule, **Snakemake** will automatically pattern-match the input files of the rule with the output files of other rules, before executing the script. In this way, **Snakemake** will recursively start a chain reaction of executions, where each rule only depends on its ancestors through its input files. Thus, the structure of rule relationships may be represented as a DAG, where an arrow from rule A to rule B indicates that an output file from A matches an input file from B. Each rule lives in an independent **Apptainer** container and the DAG relationship enables parallel executions. Note that, **Apptainer** is a container management system which requires fewer operating system privileges than, e.g., making it possible to run **Benchpress** on shared servers as opposed to **Docker** which is usually blocked for security reasons.

Snakemake has built-in support for reading configuration files in JSON format, passed as an argument to the program. The JSON file provides a simple *key-value* format which is easy to interpret and modify. This property is heavily exploited by **Benchpress**, where the JSON file gives a complete interface for the user, without modifying the rules. When the value of a key is another JSON object or a list, we call it a *section*.

At the highest level, there are two main sections, `resources` and `benchmark_setup`, described in Section 4.1 and Section 4.2, respectively. The `resources` section contains separate subsections of the available *modules* for specifying graphs (`graph`), parameters (`parameters`), data (`data`), and algorithms for structure learning (`structure_learning_algorithms`). Each module, in turn, has a list, where each element is an object defining a parameter setting, identified by a unique `id`. The `benchmark_setup` section specifies the data models (`data`) and evaluation methods (`evaluation`) a user wishes to consider for analysis. The performance evaluation of structure learning algorithms will depend not only on the chosen metric, but also on the particular graphical model of interest, and it may be measured on different spaces, e.g., CPDAGs, pattern graphs or skeletons, and these options are supported by **Benchpress**.

The module objects used in `benchmark_setup` are defined in `resources` and referenced by their corresponding `id`'s. The output files of each module are saved systematically under the *results/* directory based on the corresponding objects' values. An important consequence of this design is that an algorithm run for a specific data set will never have to be rerun, instead, the stored output files are used for the different evaluation modules.

Figure 1 shows a flowchart describing how the files and sections relate to the modules in a JSON configuration file. The notation in the Figure matches the module description in this Section. An example of such a configuration file appears in Listing 1 and is described in more detail in Section 5.1.

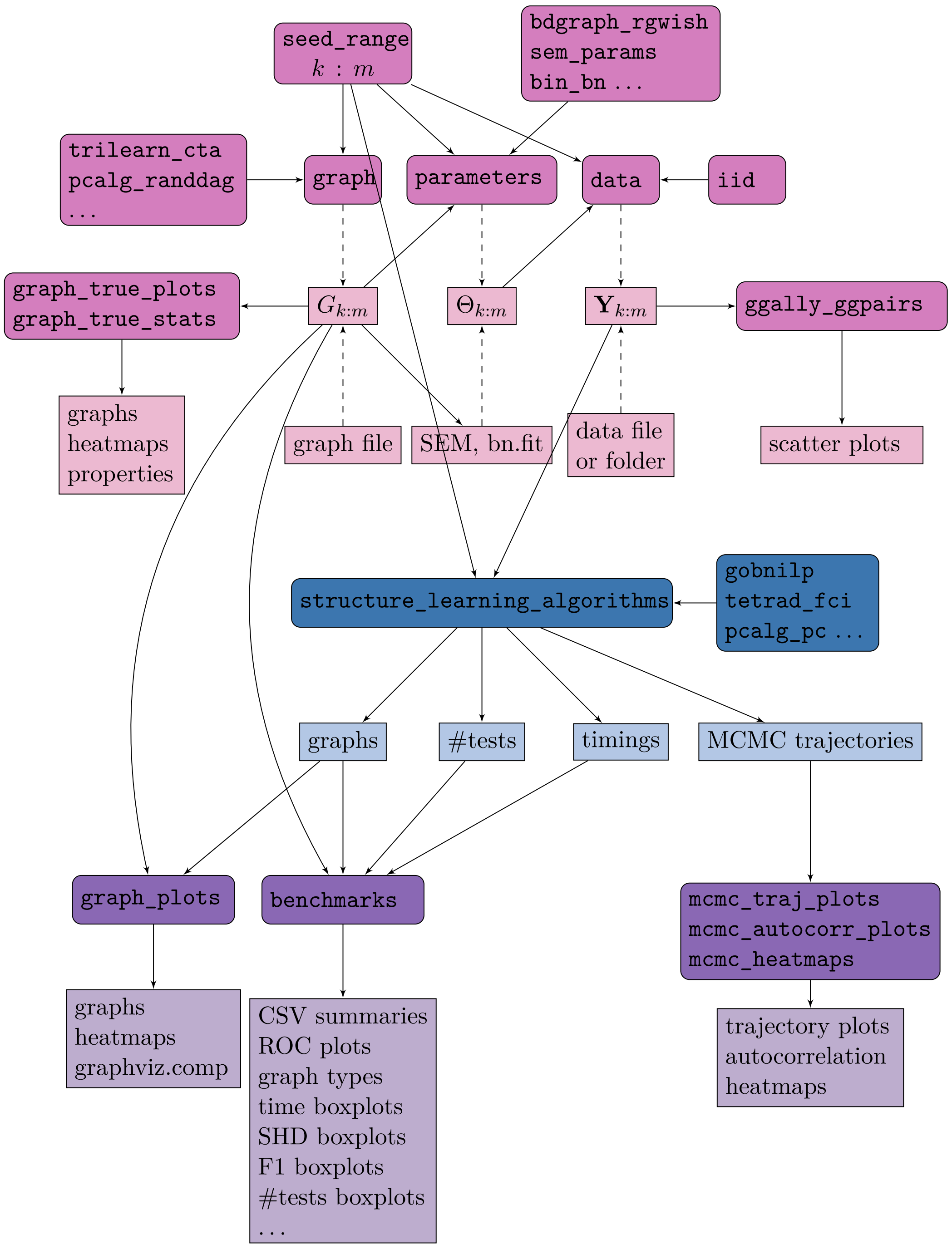

Figure 1: Flowchart for the **Benchpress** architecture describing how the files and sections (sharp rectangles) of the JSON configuration file are related to the modules (rounded rectangles with `monospace` font style). The different colors pink, blue, and purple indicate modules, files and sections related to data, structure learning, and evaluating results respectively. An arrow from a node A to another node B should be read as "B requires input from A". Thus, for any node, following the arrows in their opposite directions builds a path of the used modules or files. Dashed arrows indicate that one of the parents is required.

Method	Graph	Package	Module
Fixed graph	DAG, UG	–	`fixed_graph`
randDAG	DAG, UG	**pcalg**	`pcalg_randdag`
graph.sim function	UG	**BDgraph**	`bdgraph_graphsim`
Bandmatrix	DG	**trilearn**	`trilearn_bandmat`
CTA	DG	**trilearn**	`trilearn_cta`
Random bandmatrix	DG	**trilearn**	`trilearn_rand_bandmat`

Table 1: Graph modules.

Method	Graph	Package	Module
Fixed parameters	DAG	–	`fixed_params`
SEM parameters	DAG	**Benchpress**	`sem_params`
Binary BN	DAG	**Benchpress**	`binary_bn`
Hyper-Dirichlet	DG	**trilearn**	`trilearn_hyper-dir`
Graph intra-class	UG	**trilearn**	`trilearn_intra-class`
G-Wishart	UG	**BDgraph**	`bdgraph_rgwish`

Table 2: Parameterization modules.

Method	Graph	Package	Module
Fixed dataset(s)	All	–	`fixed_data`
gCastle i.i.d. (SEM)	DAG	**gCastle**	`gcastle_iidsim`
I.i.d. data	All	Various	`iid`

Table 3: Data modules.

4.1. Resources section (`resources`)

Tables 1–3 shows the available modules in the `graph`, `parameters`, and `data` sections. For the modules that stem from existing packages, the names are conventionally prefixed by the name of the package on which they are based. In each of these sections, there are special modules, `fixed_graph`, `fixed_params`, and `fixed_data`, enabling the user to provide graphs, parametrizations, and datasets using files. Note that, **Benchpress** already contains several standard Bayesian network models, e.g., those available at the website of **bnlearn**, including the so-called *Bayesian network repository* (Friedman, Goldszmidt, Heckerman, and Russell 1997). Below is a brief description of the other available modules. For more details, we refer to Appendix B and the **Benchpress** online documentation.

For the `graph` modules, the `bdgraph_graphsim` module uses the `graph.sim` function of the **BDgraph** package (Mohammadi and Wit 2019) to sample various types of random undirected graphs. The `pcalg_randdag` module uses the `randDAG` function of the **pcalg** package (Kalisch *et al.* 2012) to sample various types of random DAGs and undirected graphs. The `trilearn_bandmat` and `trilearn_randbandmat` modules generate undirected decomposable graphs with a band-structured adjacency matrix of a given and random width, respectively. The `trilearn_cta` module samples decomposable graphs using the so-called *Christmas tree algorithm* (CTA) (Olsson *et al.* 2022).

For the modules in the `parameters` section, the **bdgraph_rgwish** module samples the precision

	G	Θ	$\mathbf{Y}$
I	–	–	Fixed
II	Fixed	–	Fixed
III	Fixed	Fixed	Generated
IV	Fixed	Generated	Generated
V	Generated	Generated	Generated

Table 4: Data scenarios.

matrix of an undirected Gaussian graphical model from the G-Wishart distribution (Dawid and Lauritzen 1993; Atay-Kayis and Massam 2005; Lenkoski 2013). The `binary_bn` module samples the conditional probability tables of a Bayesian network with only binary variables. The `sem_params` module samples the weights of a structural equation model (SEM) Gaussian Bayesian network (see (1) in Appendix B.2). The `trilearn_hyper-dir` module samples the parameters of a multinomial decomposable graphical model from the Hyper-Dirichlet distribution (Dawid and Lauritzen 1993). The `trilearn_intra-class` module specifies the covariance matrix of a Gaussian graph intra-class model.

For the modules in the `data` section, the `iid` module is a generic module to draw independent identically distributed (IID) samples from any of the models built by proper combinations of the `graph` and `parameters` modules. The `gcastle_iidsim` module uses the `IIDSimulations` function of the **gCastle** package to draw IID samples from different types of SEM models.

The available modules in the `structure_learning_algorithms` section are listed in Table 6. For the algorithms demonstrated in the simulation studies in Section 5, we give a short overview in Appendix B.

4.2. Benchmark setup (`benchmark_setup`)

Data setup section (`data`*)*

The `data` section consists of a list of objects, each containing the `id` of a graph (`graph_id`), parameters (`parameters_id`), data (`data_id`) module object, and a tuple (`seed_range`), specifying the range of the random seeds used in the modules. For each seed number i in the specified range, a graph G_i is obtained as specified according to `graph_id`. Given G_i, the parameters in the model Θ_i are obtained according to `parameters_id`. A data matrix, $\mathbf{Y}_i = (Y^j_{1:p})^n_{j=1}$, is then sampled from (G_i, Θ_i) according to the model and `data_id`. When combining modules from the different sections, it is important to ensure that (G_i, Θ_i) is a compatible pair, e.g., if Θ_i represents the parameters of Bayesian network then G_i is required to be a DAG.

By using the modules for fixed files, we can build models with increased flexibility. The different data sources provided by **Benchpress** can be summarized in five scenarios shown in Table 4. Scenario I is the typical scenario for data analysts, where users provide one or more datasets by hand. Scenario II is similar to Scenario I, where the difference is that in addition, the user provides the true graph underlying the data. This situation arises, e.g., when replicating a simulation study from the literature, where both the true graph and the dataset are given. Scenarios III-V are pure benchmarking scenarios, where either all of the graphs, parameters, and data are generated (V), or the graphs (III, IV) and possibly parameters (III) are specified by the user.

Evaluation	Module
Benchmarks	`benchmarks`
Pairs plot	`ggally_ggpairs`
Graph plots	`graph_plots`
True graph plots	`graph_true_plots`
True graph properties	`graph_true_stats`
MCMC auto-correlation	`mcmc_autocorr_plots`
MCMC mean graphs	`mcmc_heatmaps`
MCMC trajectories	`mcmc_traj_plots`

Table 5: Evaluation modules.

Note that, when a filename is used as `data_id`, since the data is fixed, `seed_range` should be set to `null`. However, depending on the evaluation module used, the `graph_id` could be either `null` or the filename of the true graph underlying the data. For example, the `benchmarks` module requires that `graph_id` is set to a proper `id` for a graph module object, while it is not a requirement for the `adjmat_plots` module. When the value of `data_id` is a directory, the other fields should be set to `null`.

Evaluation section (`evaluation`*)*

Table 5 shows the modules available in the `evaluation` section. The figures for each module are saved systematically in `results/` based on the parameterization of the module used and copied to `results/output/` for easy reference. Further details are provided in Appendix B.

The `benchmarks` module provides timings and comparisons using standard benchmarking metrics. The results are summarized in e.g., *box plots* and *receiver operating characteristic* (ROC)-type curves. In addition to the figures produced, the raw data is saved in *comma separated values* (CSV) files which could be analyzed externally. The `ggally_ggpairs` module uses the `ggpairs` function of the **GGally** package (Emerson *et al.* 2013) to visualize the data in pairwise scatter plots. The `graph_plots` module plots and saves the estimated graphs and adjacency matrices. If the true graph is available (scenarios II-V in Table 4) it also compares the true to the estimated graphs using the `graphviz.compare` function from the **bnlearn** package (Scutari 2010). The `graph_true_plots` module plots the true underlying graphs and corresponding adjacency matrices. The `graph_true_stats` module computes and plots properties of the true underlying graphs. For the MCMC algorithms, the following three special evaluation modules are available. The `mcmc_heatmaps` module estimates posterior edge probabilities and plots them in heatmaps using the **seaborn** package (Waskom 2021). The `mcmc_traj_plots` module plots the value of a given functional for the graphs in an MCMC trajectory. The currently supported functionals are the number of edges for the graphs and the scores. The `mcmc_autocorr_plots` module plots the auto-correlation of a functional of the graphs in a MCMC trajectory.

5. Benchpress in practice

We demonstrate the functionalities of **Benchpress** with seven examples for benchmarking structure learning algorithms for Bayesian networks. We consider the pure benchmarking setting for both binary and continuous data types as well as a fixed data scenario (Section 5.2). For performance evaluation and visualization, we use the modules `benchmarks`, `graph_true_stats`, `ggally_ggpairs`, and `graph_plots`. The title rows of each sub-figure describe the settings for the graph, parameters and data modules, and the number of datasets used.

We use the `benchmarks` module to show scatter plots of the individual results in terms of ROC type curves, where median FP/P is plotted against the median TP/P together with estimated 5%-95% percentiles in ROC type figures (see Appendix A.1 for definitions). Since not all methods support the same test procedures or scores, we have chosen the default settings for some of the algorithms. The parameter values are selected so as to indicate how the performance changes. However, some curves are shorter than would be desired due to range limits for the parameters in the programs used.

For *binary data* we use the *Bayesian Dirichlet likelihood-equivalence* (BDe) score (Heckerman, Geiger, and Chickering 1995) in the score-based methods while varying the equivalent sample size parameter (Silander, Kontkanen, and Myllymäki 2007). The benchmarking setup considers the following score-based algorithms: BOSS (`boss-bdeu`), GRaSP (`grasp-bdeu`), HC (`hc-bde`), Tabu (`tabu-bde`), ASOBS (`asobs-bdeu`), GOBNILP (`gobnilp-bde`), Iterative search (`itsearch-bde`), and order MCMC with the end space of `itsearch-bde` as start space (`omcmc-bde`). Furthermore, we include the constraint-based PC algorithm with the G^2-test (`pc-binCItest`) and the hybrid method MMHC (`mmhc-bde-mi`) with the *mutual information* test and the BDe score. The varying parameter to draw ROC-type curves for all constraint-based methods is the significance level for the independence tests.

For the *continuous datasets*, we use either a Bayesian score or a penalized likelihood-based score in the score-based methods. The benchmarking setup in this case includes HC (`hc-bge`), Tabu (`tabu-bge`), GOBNILP (`gobnilp-bge`), Iterative search (`itsearch-bge`), and order MCMC using the end space of `itsearch-bge` as start space (`omcmc-bge`) with the *Bayesian Gaussian likelihood-equivalence* (BGe) score (Geiger and Heckerman 1994, 2002; Kuipers, Moffa, and Heckerman 2014), and varying levels of the prior parameter. Furthermore we include the FGES (`fges-sem-bic`), BOSS (`boss-sem-bic`), and GRaSP (`grasp-sem-bic`) with the *structural equation model Bayesian information criterion* (SEM-BIC) score (Glymour and Scheines 1986), and varying levels of the penalty discount. We also include the NO TEARS algorithm (`notears-l2`) with the L_2 penalty. For constraint-based methods we include the PC algorithm (`pc-gaussCItest`), dual PC algorithm (`dualpc`), and MMHC (`mmhc-bge-zf`) with the *Fisher's z-transformation* test of partial correlations (Edwards 2012) with varying significance levels.

5.1. Comparative study between the PC and the dual PC algorithm

We start with a simple demonstration comparing just two algorithms side-by-side and a small-scale simulation study from data scenario V with the PC and the dual PC algorithms. We consider data from 10 random Bayesian network models $\{(G_i, \Theta_i)\}_{i=1}^{10}$, where each graph G_i has $p = 80$ nodes and is sampled using the `pcalg_randdag` module. The parameters Θ_i are sampled from the random linear Gaussian SEM using the `sem_params` module (Appendix B.2) with $a = 0.25, b = 1, \mu = 0$ and $\sigma = 1$. We draw a standardized dataset $\mathbf{Y}_i$ of size $n = 300$ from each model using the `iid` module. Listing 1 shows the content of the JSON configuration file (`config/paper_pc_vs_dualpc.json`) for this study.

```
{
  "benchmark_setup": {
    "data": [
      {
        "graph_id": "avneighs_p20",
        "parameters_id": "SEM",
        "data_id": "standardized",
        "seed_range": [
          1,
          10
        ]
      }
    ],
    "evaluation": {
      "benchmarks": {
        "filename_prefix": "paper_pc_vs_dualpc/",
        "show_seed": false,
        "errorbar": true,
        "errorbarh": false,
        "scatter": true,
        "path": true,
        "text": false,
        "ids": [
          "pc-gaussCItest",
          "dualpc"
        ]
      },
      "graph_true_plots": true,
      "graph_true_stats": true,
      "ggally_ggpairs": false,
      "graph_plots": [
        "pc-gaussCItest",
        "dualpc"
      ],
      "mcmc_traj_plots": [],
      "mcmc_heatmaps": [],
      "mcmc_autocorr_plots": []
    }
  },
  "resources": {
    "data": {
      "iid": [
        {
          "id": "standardized",
          "standardized": true,
          "n": 300
        }
      ]
    },
    "graph": {
      "pcalg_randdag": [
        {
          "id": "avneigs4_p20",
          "max_parents": 5,
          "n": 20,
          "d": 4,
          "par1": null,
          "par2": null,
          "method": "er",
          "DAG": true
        }
      ]
    },
    "parameters": {
      "sem_params": [
        {
          "id": "SEM",
          "min": 0.25,
          "max": 1
        }
      ]
    },
    "structure_learning_algorithms": {
      "dualpc": [
        {
          "id": "dualpc",
          "alpha": [
            0.001,
            0.05,
            0.1
          ],
          "skeleton": false,
          "pattern_graph": false,
          "max_ord": null,
          "timeout": null
        }
      ],
      "pcalg_pc": [
        {
          "id": "pc-gaussCItest",
          "alpha": [
            0.001,
            0.05,
            0.1
          ],
          "NAdelete": true,
          "mmax": "Inf",
          "u2pd": "relaxed",
          "skelmethod": "stable",
          "conservative": false,
          "majrule": false,
          "solveconfl": false,
          "numCores": 1,
          "verbose": false,
          "indepTest": "gaussCItest",
          "timeout": null
        }
      ]
    }
  }
}
```

Listing 1: The JSON configuration file `paper_pc_vs_dualpc.json` to define a small comparison between the PC and dual PC algorithms.

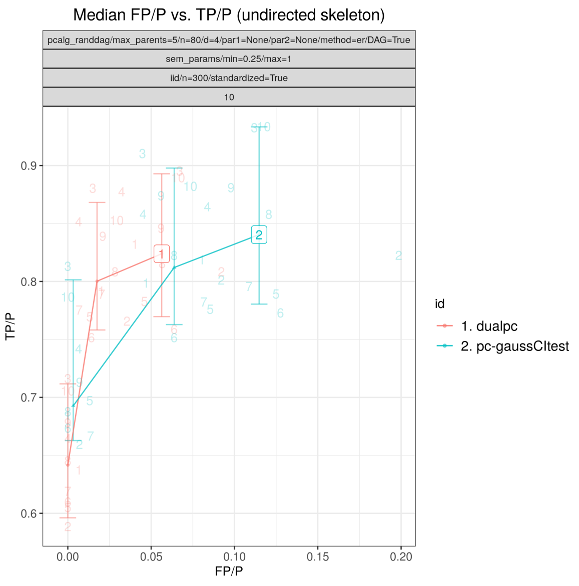

(a)

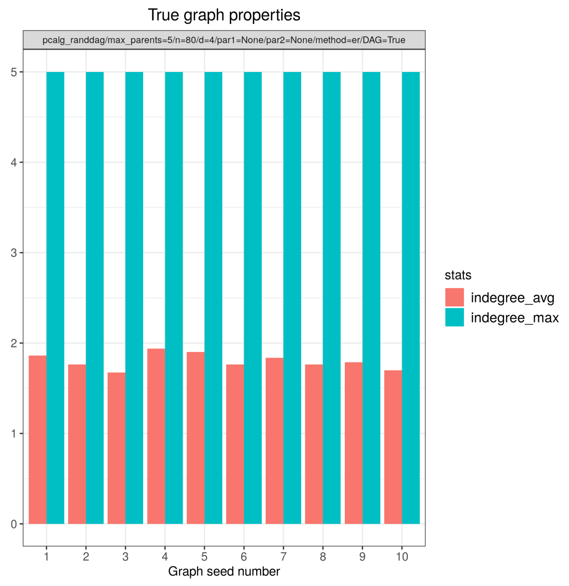

(b)

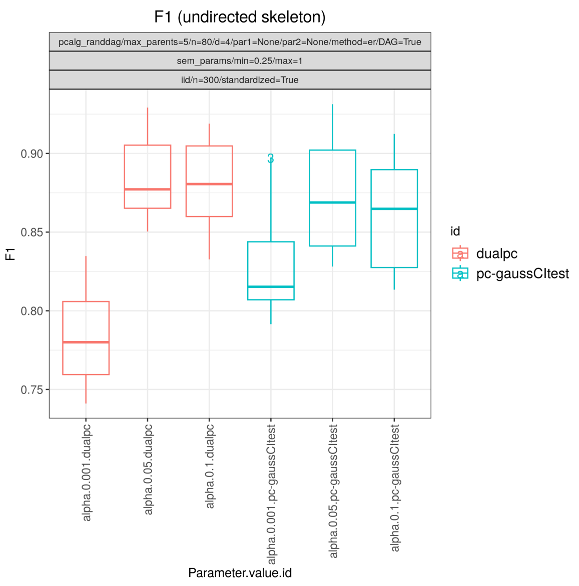

(c)

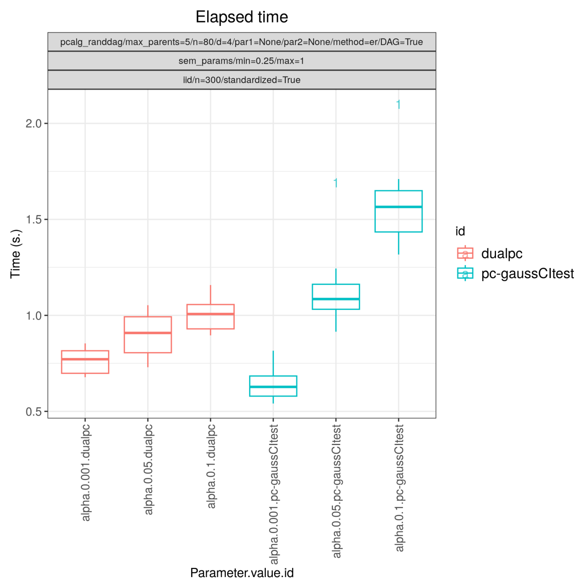

(d)

Figure 2: This figure shows results for a comparative study between the PC `pcalg_pc` and the dual PC `dualpc` algorithm. In (2a) FP/P (and median FP/P) is plotted against TP/P (and median TP/P) in a ROC-type figure based on the `graph`, `parameters`, and `data` modules used. The parameter values are selected so as to indicate how the performance changes. The upper and lower bars in the plots show the estimated 5% and 95% quantiles of the TP/P for each module setting. F_1 scores based on the graph skeletons and computational times are visualized by box-plots in (2c) and (2d), respectively, where outliers are indicated by the corresponding seed number. Graph properties calculated from the underlying true graphs are shown in (2b) and provided by the `graph_true_stats` module. All the plots are based on graphs and datasets corresponding to 10 different seed numbers.

Figure 2 shows results from the `benchmarks` and the `graph_true_stats` module, where we have focused on the undirected skeleton for evaluations since this is the part where the algorithms mainly differ. More specifically, from Figure 2a, showing the FP/P and TP/P, we see that the dual PC has superior performance for significance levels $\alpha = 0.05, 0.01$. Apart from the curves, the numbers in the plot indicate the seed number of the underlying dataset and models for each run. We note that the model with seed number 3 seems to give good results for both algorithms and looking into Figure 2b, we note that the graph with seed number 3 corresponds to the one with the lowest graph density ($|E|/|V|$). The box plots from Figure 2d show the computational times for the two algorithms, where the outliers are labeled by the model seed numbers. We note, e.g., that seed number 1 gave longer computational time for the standard PC algorithm and from Figure 2b we find that the graph with seed number 1 has relatively high graph density. The conclusion of the F_1 score plot in Figure 2c is in line with the FP/P vs. TP/P results from Figure 2a.

5.2. Biological dataset with fixed DAG

Next, we consider the data from Sachs, Perez, Pe'er, Lauffenburger, and Nolan (2005) containing cytometry measurements of 11 phosphorylated proteins and phospholipids, which has become a common benchmarking example in this field since the true underlying graph is regarded as known, and as such we include a wider range of algorithms in the comparison. The dataset consists of 7644 measurements in total, from nine different perturbation conditions, each defining a unique intervention scheme. Sachs *et al.* (2005) removed any data points that fell more than three standard deviations away from the mean. The data were then discretized on three levels. They also use bootstrapping methodologies and exploit the interventional dataset to determine the causal directions of edges.

However, since the purpose here is to benchmark algorithms suited for observational data, we consider only the first two interventions, referred to as *(anti-CD3/CD28)* and *(anti-CD3/CD28 + ICAM-2)* as only these interventions are expected to be independent of the nodes in the network and just activate the T-cells generally. **Benchpress** also provides support for interventional data (Hauser and Bühlmann 2012; Wang, Solus, Yang, and Uhler 2017; Kuipers and Moffa 2025) through the `pcalg_gies` module (Hauser and Bühlmann 2012), though we focus on the observational case here. We show results for the (logged and standardized version of) the second dataset (*anti-CD3/CD28 + ICAM-2*) with 902 observations since the graphs estimated from this dataset were in general closer to the gold standard network. The data are visualized in Figure 3 with independent and pairwise scatter plots using the `ggally_ggpairs` module.

Listing 2 shows the object in the `data` section of the config file defining the data setup. This setup falls into data Scenario II of Table 4 since the `graph_id` is set to the filename of the graph. For Scenario I, when the underlying graph is unknown, `graph_id` would be set to `null`. The full JSON specification for this study is found in `config/paper_sachs.json`.

Figure 4a shows SHD based on the CPDAG and Figure 4b the F_1 score based on the undirected skeleton from 11 algorithms with different parametrizations, produced by the `benchmarks` module. From these figures we can directly conclude that all algorithms have a parameterization that gives the minimal SHD of 9 and maximal F_1 score of 0.67. Figure 5a and Figure 5b show the adjacency matrix and DAG plots, respectively, produced by the `graph_plots` module of the DAG estimated by the `tetrad_fges` module. Figure 6 shows the pattern graph of

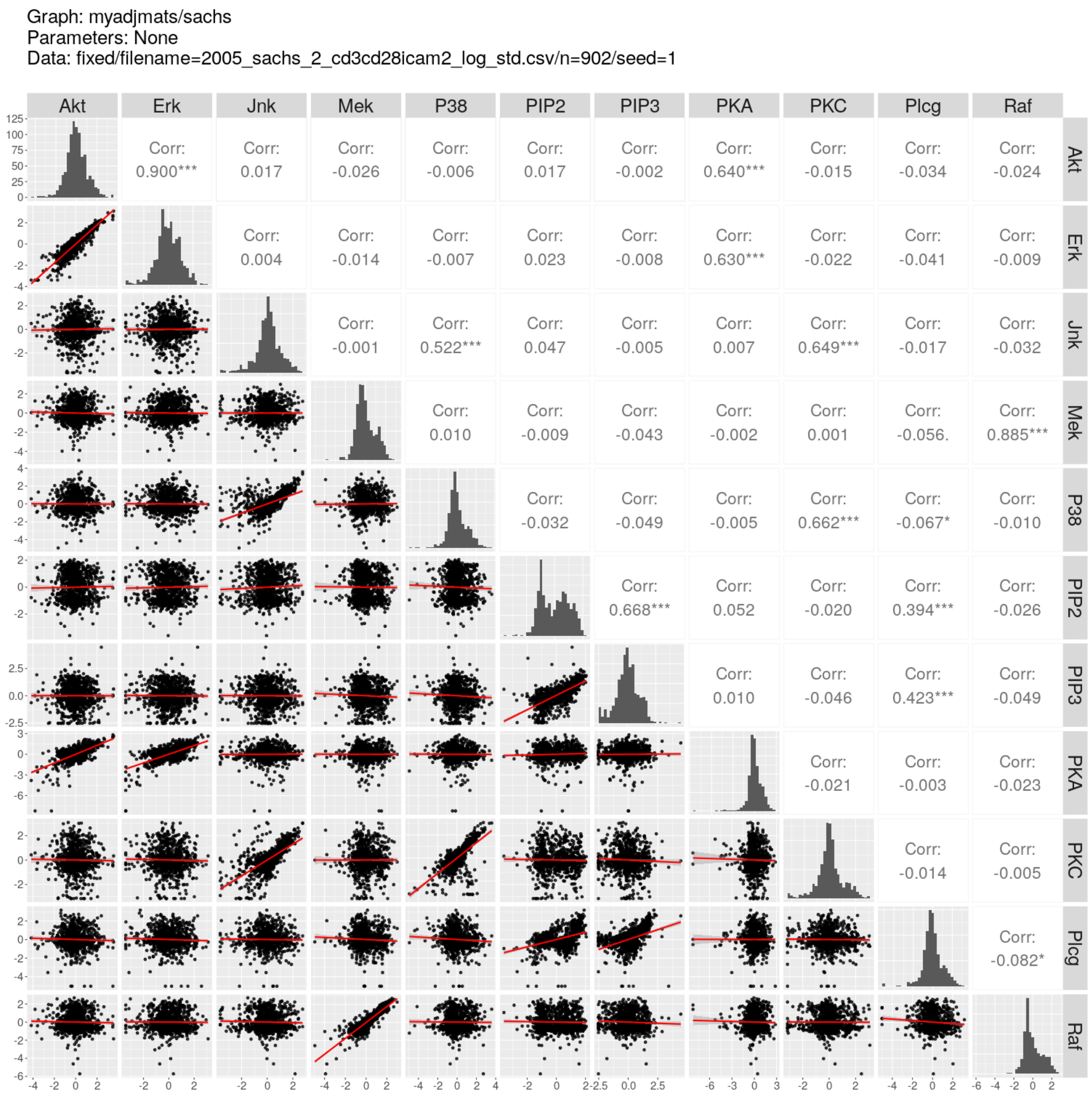

Figure 3: Scatter plots of the logged and standardized data from the second experiment in Sachs *et al.* (2005) by the `ggally_ggpairs` module.

```
{
  "graph_id": "sachs.csv",
  "parameters_id": null,
  "data_id": "2005_sachs_2_cd3cd28icam2_log_std.csv",
  "seed_range": null
}
```

Listing 2: Scenario II data object for the transformed second dataset from Sachs *et al.* (2005).

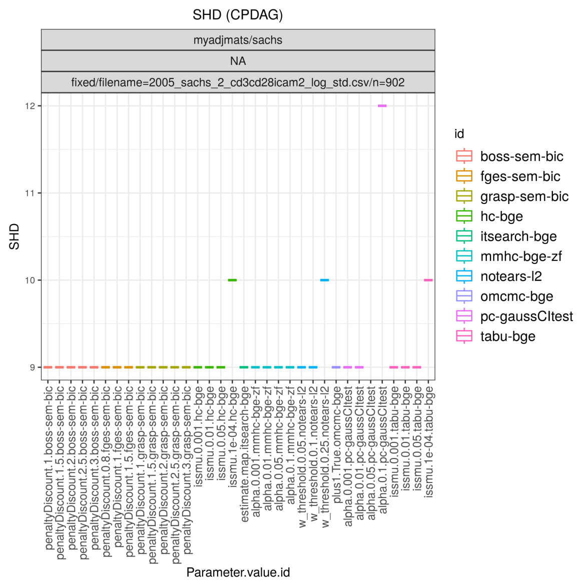

(a)

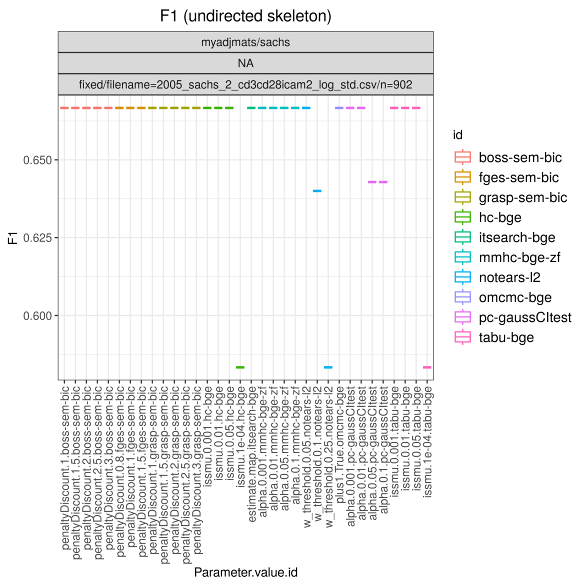

(b)

Figure 4: SHD (4a) based on the CPDAG and F_1 score (4b) based on the skeleton produced by the **benchmarks** module.

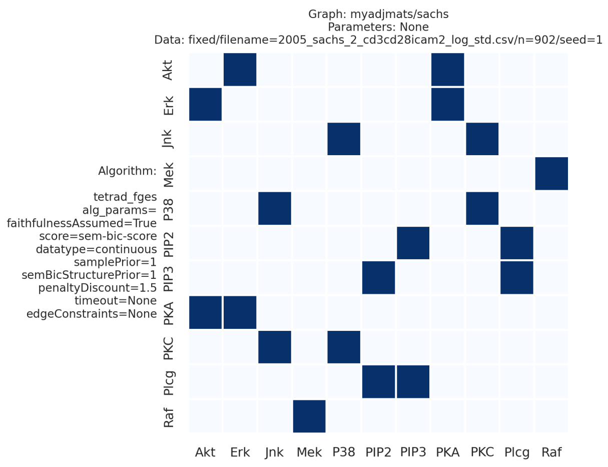
Graph: myadjmats/sachs
Parameters: None
Data: fixed/filename=2005_sachs_2_cd3cd28icam2_log_std.csv/n=902/seed=1

Algorithm:

tetrad_fges
alg_params=
faithfulnessAssumed=True
score=sem-bic-score
datatype=continuous
samplePrior=1
semBicStructurePrior=1
penaltyDiscount=1.5
timeout=None
edgeConstraints=None

(a)

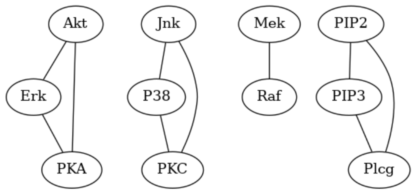

(b)

Figure 5: Adjacency matrix (5a) and graph (5b) plots produced by the `graph_plots` module for the FGES estimate.

both the true (Figure 6a) and an estimated CPDAG (Figure 6b) obtained by the `tetrad_fges` module, where the black edges are correct in both subfigures. The missing and incorrect edges are colored in blue and red respectively in Figure 6b.

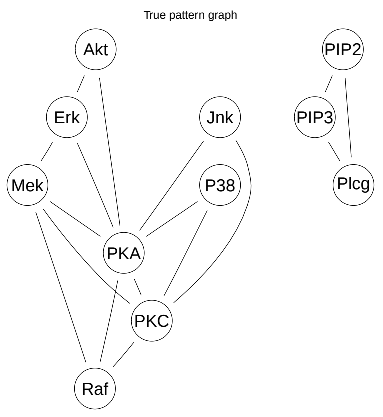

(a)

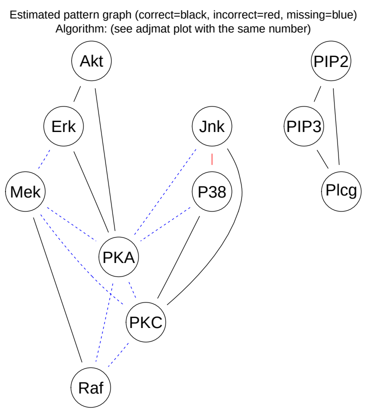
Estimated pattern graph (correct=black, incorrect=red, missing=blue)
Algorithm: (see adjmat plot with the same number)
Akt
PIP2
Erk
Jnk
PIP3
Mek
P38
Plcg
PKA
PKC
Raf

(b)

Figure 6: True pattern graph (6a) along with a comparison to the estimated pattern graph (6b), using the `graph_plots` module for the FGES estimate shown in Figure 5, with parameters as in Figure 5a.

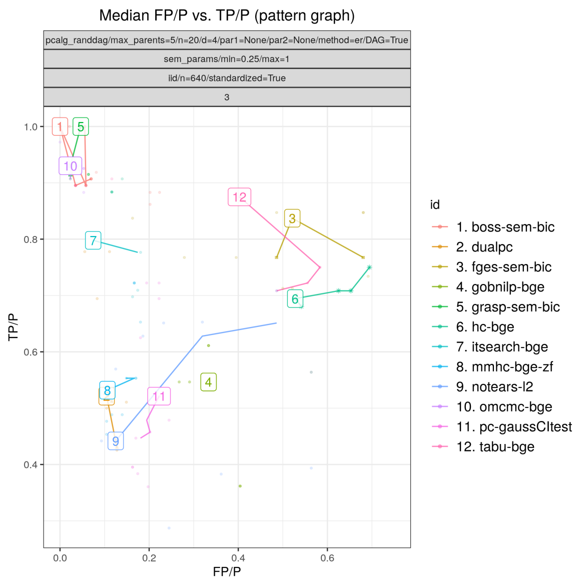

(a)

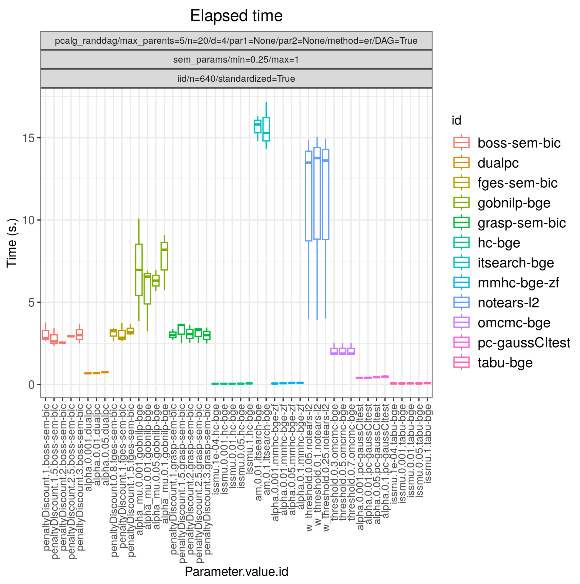

(b)

Figure 7: ROC type curves (7a) and timing (7b) from the `benchmarks` module (see caption of Figure 2) evaluated on 20 datasets from a small scale Linear Gaussian SEM with random weights and random DAGs.

5.3. Linear Gaussian SEM with random weights and random DAGs

In the present study we consider a broader simulation over 11 algorithms in a similar Gaussian data setting as in Section 5.1, with the additional difference that the number of nodes is reduced to 20 and the number of seeds is increased to 20. This study took about 40 minutes to finish on a MacBook Pro 2016 with 3.1 GHz Dual-Core Intel Core i5. The full JSON specification for this study is found in `config/paper_er_sem_small.json`.

Figure 7a shows the TP/P and FP/P based on pattern graphs and Figure 7b shows the computational times. We can directly observe that BOSS (`boss-sem-bic`), GRaSP (`grasp-sem-bic`), and the order MCMC (`omcmc-bge`) have very good performance, though they tend to also have longer computational time. Apart from this, the results of Figure 7a may be partitioned into two regions, FGES (`fges-sem-bic`), HC (`hc_sem-bic`), and Tabu (`tabu-bge`) having higher values for both TP/P and FP/P and the rest having lower values for both TP/P and FP/P.

5.4. Binary valued Bayesian network with random parameters and DAG

In this example, we study a binary-valued Bayesian network, where both the graph G and the parameters Θ are regarded as random variables. More specifically, we consider 100 models $\{(G_i, \Theta_i)\}_{i=1}^{100}$, where each G_i is sampled according to the Erdős-Rényi random DAG model using the `pcalg_randdag` module (Appendix B.1), where the number of nodes is $p = 80$, the average number of neighbors (parents) per node is 4 (2) and the maximal number of parents per node is 5. The parameters Θ_i are sampled using the `bin_bn` module (Appendix B.2) and restricting the conditional probabilities within the range $[0.1, 0.9]$. From each model, we draw one dataset $\mathbf{Y}_i$, of size $n = 320$ using the `iid` module. The full JSON specification for this study is found in `config/paper_er_bin.json`.

Figure 8a shows the ROC type curves for the algorithms considered for the data generated as described above. The algorithms standing out in terms of low SHD in combination with low best median FP/P (< 0.12) and higher best median TP/P (> 0.5) are BOSS (`boss-bdeu`), GRaSP (`grasp-bdeu`), FGES (`fges-bdeu`), followed by iterative order MCMC (`omcmc-bde`).

5.5. Linear Gaussian SEM with random weights and random DAG

In this example, we again study Gaussian random Bayesian networks, of size $p = 80$ and with 100 repetitions $\{(G_i, \Theta_i)\}_{i=1}^{100}$. We use the same module configurations as in Sections 5.1 and 5.3 and draw one standardized dataset $\mathbf{Y}_i$, of size $n = 320$ from each of the models using the `iid` module. The full JSON specification for this study is found in `config/paper_er_sem.json`.

Figure 8b shows ROC type results for all the algorithms considered for the data generated as described above. The constraint-based methods PC (`pc-gaussCItest`) and dual PC (`dualpc`) have comparable and lower best median TP/P (< 0.7) than the remaining algorithms. In terms of achieving high TP/P (> 0.9) iterative order MCMC (`omcmc-bge`) and iterative search MCMC (`itsearch-bge`) followed by BOSS (`boss-sem-bic`) and GRaSP (`grasp-sem-bic`) stand out with near perfect performance, i.e., SHD ≈ 0. Among the other algorithms GOBNILP (`gobnilp-bge`) performs next best with TP/P ≈ 0.85 and FP/P ≈ 0.08 followed by FGES (`fges-sem-bic`).

5.6. Bayesian network with random parameters and fixed DAG

In this example, we study a random binary Bayesian network where the graph G is fixed and the associated parameters Θ are regarded as random. More specifically, we consider 100 models $\{(G, \Theta_i)\}_{i=1}^{100}$, where the graph structure G is that of the well known Bayesian network *HEPAR II* (`hepar2.csv`), first introduced in Onisko (2003). This graph has 70 nodes and 123 edges and has become one of the standard benchmarks for evaluating the performance of structure learning algorithms. The maximum number of parents per node is 6 and we

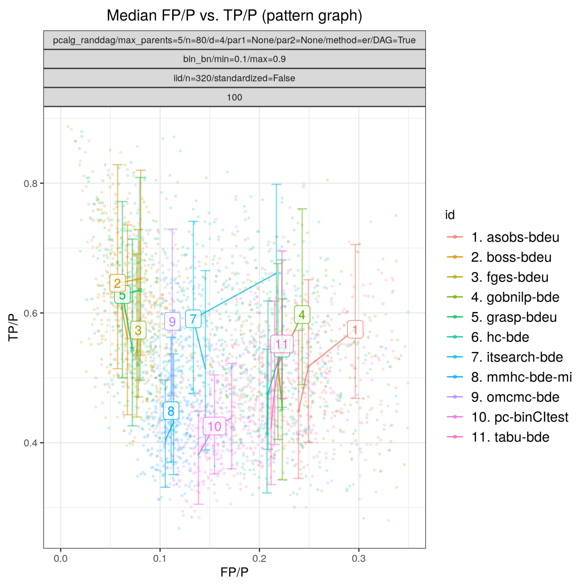

(a) Binary valued Bayesian network with random parameters and random DAG.

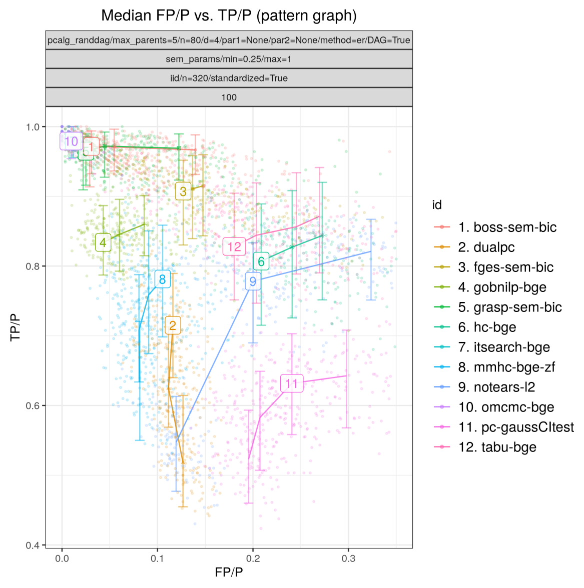

(b) Linear Gaussian SEM with random weights and random DAG.

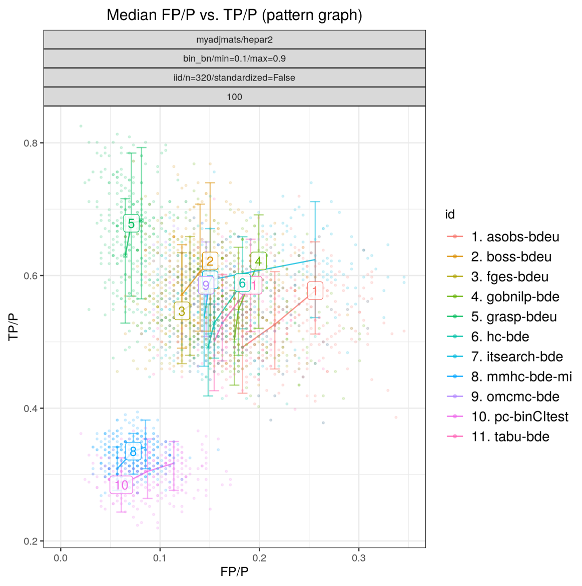

(c) Binary valued Bayesian network with random parameters and (fixed) HEPAR II DAG.

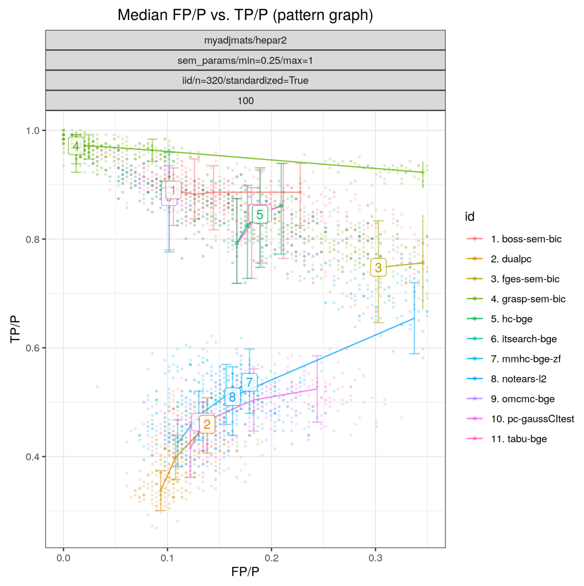

(d) Linear Gaussian SEM with random weights and (fixed) HEPAR II DAG.

Figure 8: ROC type curves (see the caption of Figure 2 for further details) showing the FP/P and TP/P evaluated on 100 datasets from 4 different Bayesian network models.

sample the parameters Θ_i using the `bin_bn` module (Appendix B.2), in the same manner as described in Section 5.4. From each model we draw, as before, one dataset $\mathbf{Y}_i$ of sample size $n = 320$, using the `iid` module. The full JSON specification for this study is found in `config/paper_hepar2_bin.json`.

Figure 8c shows the ROC type curves for this scenario. The algorithms appear to divide between two groups with respect to their performance in terms of TP/P. Constraint-based methods including PC (`pc-binCItest`), and MMHC (`mmhc-bde-mi`) appear to cluster in the lower scoring region (TP/P < 0.5). Score-based methods on the other hand seem to concentrate in the higher-scoring region (TP/P > 0.5). The best performing algorithm is clearly GRaSP (`grasp-bdeu`) followed by a group of algorithms including FGES (`fges-bdeu`), BOSS (`boss-bdeu`), iterative order MCMC (`omcmc-bde`), and iterative search MCMC (`itsearch-bde`), all with FP/P ≈ 0.15.

5.7. Linear Gaussian SEM with random weights and fixed DAG

In this example we draw again 100 models $\{(G, \Theta_i)\}_{i=1}^{100}$, where G corresponds to the HEPAR II network (`hepar2.csv`), and Θ_i are the parameters of a linear Gaussian SEM sampled using the `sem_params` module (Appendix B.2) with the same settings as in Section 5.5. From each of the models (G, Θ_i), we draw one standardized dataset $\mathbf{Y}_i$ of size $n = 320$ (`iid`). The full JSON specification for this study is found in `config/paper_hepar2_sem.json`.

The ROC-type curves of Figure 8d highlight that GRaSP (`grasp-sem-bic`) again separates itself from the rest of the best algorithms with the more favorable performance. Next follows order MCMC (`omcmc-bge`), iterative search MCMC (`itsearch-bge`), and BOSS (`boss-sem-bic`). In terms of best median TP/P (> 0.8) only HC (`hc-bge`) and Tabu (`tabu-bge`) display similar performances, while performing considerably worse with respect to median FP/P (≈ 0.1 vs ≈ 0.17).

6. Installation and usage

6.1. Requirements

Benchpress can run either natively on Linux systems or via *Windows subsystem for Linux* (WSL) on Windows systems. Alternatively one can run through **Docker**, which enables it also for macOS. In either alternative, **Benchpress** should be cloned from the **git** repository `https://github.com/felixleopoldo/benchpress` which should be set as the working directory:

```
$ git clone https://github.com/felixleopoldo/benchpress.git
$ cd benchpress
```

Linux (native)

Running the **Benchpress** workflow natively requires **Snakemake** ($\geq$ 7.30.1) and **Apptainer** (Kurtzer *et al.* 2017) to be installed on a Linux system. See the documentation of **Snakemake** and **Apptainer** for specific installation instructions. If **Snakemake** is installed with **conda** (**Anaconda** Inc. 2016, as suggested in **Snakemake**'s documentation) in an environment named, e.g., `snakemake`, it should be activated by:

```
$ conda activate snakemake
```

Windows (using WSL)

To install WSL, open PowerShell or Windows Command Prompt in administrator mode and type the following command and follow the instructions:

```
wsl --install
```

To start WSL type:

```
wsl
```

Benchpress can then be installed in the same way as for native Linux by following the instructions above. The files produced by **Benchpress** in WSL can be found under your networks in Windows.

Linux/macOS/Windows (using Docker)

For this alternative, the only requirement is **Docker**, which can be installed following the instructions on their official website. The **Snakemake** commands are then executed from an interactive shell of the **Docker** image `bpimages/snakemake:v9.7.1`, where both **Snakemake** and **Apptainer** are installed. The working directory (the `benchpress` directory) is a shared volume and is mounted in the `/mnt` folder. The command is:

```
$ docker run -it -w /mnt --privileged -v $(pwd):/mnt \
  bpimages/snakemake:v9.7.1
```

Windows users should substitute `$(pwd)` for the absolute path to the `benchpresss` folder.

6.2. Usage

Configuration files are executed through **Snakemake** commands with `--sdm apptainer`. For example, the following command will use all the available cores to run the config file `config/config.json`

```
$ snakemake --cores all --sdm apptainer --configfile config/config.json
```

For alternative use cases, e.g., execution in the cloud or on a grid, we refer to the documentation of **Snakemake**.

7. New modules

One of the main strengths of **Benchpress** is that the modular design provides a flexible framework to integrate new modules into any of the module sections. Next, we demonstrate how to add a new module, update the documentation, and push it upstream.

7.1. Adding new modules

In this section, we show an example of how to add a new structure learning module. Adding parameterization and data modules is done similarly. To get started, copy the template module `new_alg` to a new module that we name `mymod`. To do this (macOS/Linux) type the following command from the `benchpress` folder:

```
$ cp -r resources/module_templates/new_alg \
  workflow/rules/structure_learning_algorithms/mymod
```

```
rule:
   name:
       module_name
   input:
       data = alg_input_data()
   output:
       adjmat = alg_output_adjmat_path(module_name),
       time = alg_output_time_path(module_name),
       ntests = alg_output_ntests_path(module_name)
   container:
       "docker://bpimages/sandbox:1.0"
   script:
       "script.R"
```

Listing 3: **Snakemake** rule file `rule.smk` of the `new_alg` template.

```
source("workflow/scripts/utils/helpers.R")

myalg <- function() {
   data <- read.csv(snakemake@input[["data"]], check.names = FALSE)
   start <- proc.time()[1]
   p <- ncol(data)
   set.seed(as.integer(snakemake@wildcards[["seed"]]))

   # Naive algorithm start
   cutoff <- as.numeric(snakemake@wildcards[["cutoff"]])
   adjmat <- matrix(runif(p * p), nrow = p, ncol = p) > cutoff
   adjmat <- 1 * (adjmat | t(adjmat))
   diag(adjmat) <- 0
   # Naive algorithm end

   totaltime <- proc.time()[1] - start
   colnames(adjmat) <- names(data) # Get the labels from the data
   write.csv(adjmat, file = snakemake@output[["adjmat"]],
             row.names = FALSE, quote = FALSE)
   write(totaltime, file = snakemake@output[["time"]])
   write("None", file = snakemake@output[["ntests"]])
}

add_timeout(myalg)
```

Listing 4: The R script `script.R` for the `new_alg` template module.

```
{
    "id": "testing_myalg",
    "cutoff": 0.8,
    "timeout": null
}
```

Listing 5: Example JSON object for the `new_alg` template module.

This will create the new module `mymod` (in `<path-to>/mymod/`) which is ready to be used alongside the existing ones.

The module contains files that are needed for the module's functionality and documentation. It is pre-configured in `rule.smk` (Listing 3, Line 13) to run the template `script.R` (Listing 4), which implements an algorithm that merely samples a random binary symmetric matrix. The `snakemake` variable, used in `script.R`, is an object that provides access to the `input` (Listing 3, Line 4) and `output` (Listing 3, Line 6) fields of `rule.smk` (Listing 4, Lines 18, 20, and 21) and to the module's JSON object keys through the `wildcards` list (Listing 4, Lines 7, 10). Note that, the keys of the `wildcards` list are directly inherited from the keys of the JSON object used in the config file, see Listing 5 for an example. The `wildcards` list also contains the random seed number (Listing 4, Line 7) stemming from the `seed_range` specified in the `data_setup` section of the config file.

In the simplest case when adapting the module to your algorithm, you essentially only have to alter the rows between Lines 9–14 in Listing 4 and the keys of the JSON object. The module will by default run in a container based on the **Docker** image `"bpimages/sandbox:1.0"`, where both R and Python are installed. This may be changed to any suitable image that **Snakemake** supports, e.g., a **Docker** image at *Docker Hub*. To force local execution, which might be desirable when developing a new algorithm, the `container` field of `rule.smk` (Listing 3, Line 11) should be set to `None`.

Note that the actual algorithm is embedded in the function called `myalg`, which is passed to the function `add_timeout`. This enables a timeout functionality, which writes an empty file if the algorithm has not finished before `timeout` seconds, specified in the config file. However, if the algorithm can produce a graph estimate after a pre-specified amount of time, that graph should preferably be written.

The module template also contains a Python script, `script.py`, which could directly replace `script.R` in `rule.smk` (Listing 3, Line 13). For other languages and further details about customizing **Snakemake** rules, we refer to **Snakemake**'s official documentation.

7.2. Documentation

The documentation for a module can easily be generated based on information provided by the files in the modules folder. The files and their purpose are described next. The file `schema.json` is a JSON schema for restricting the fields of a module's JSON objects, forcing the user to provide valid input parameters. It also allows the developer to provide a description of each of the input parameters. The file `info.json` should be filled with meta-information about the module, in terms of, e.g., version number, links to the documentation, and the type of graph the module supports. `bibtex.bib` is a BibTeX file where the references, relevant to the module can be added. `docs.rst` is a documentation file in reStructuredText format that should contain an overview of the module and relevant information.

To generate an HTML version of the documentation using **sphinx**, the following commands should be executed from the `benchpress` directory (macOS/Linux):

```
$ pip install -r docs/source/requirements.txt
$ cd docs
$ chmod u+x render_docs.sh
$ ./render_docs.sh
$ make html
```

The documentation can be seen by opening `docs/build/html/index.html` with a web browser.

7.3. Contributing

The instructions above show how to integrate a new module into **Benchpress**. To add a module to the **Benchpress** official repository, the module should run on a **Docker** or **Apptainer** image available at, e.g., Docker Hub. Publishing modules (or any contributions) to **Benchpress** is done by creating a so-called fork of the **Benchpress**'s GitHub repository (`https://github.com/felixleopoldo/benchpress`) and creating a so-called pull request.

7.4. Reproducibility

All the pieces of information used to build the benchmarks in **Benchpress** are saved as files that are easily accessible. For all the simulations, **Benchpress** uses fixed random seeds to ensure that the code will produce the same results again. Using **Docker** and **Apptainer** makes it easy to reproduce results on essentially any modern computer. When a new module is published, we encourage the developer to attach one or more config files that highlight important properties of the modules along with a few example output figures in `docs.rst`.

8. Conclusions

Benchpress provides a novel **Snakemake** workflow for scalable and reproducible execution and benchmarking of structure learning algorithms. **Snakemake**'s support for running containerized software through **Apptainer** together with the simple data and graph representation enables **Benchpress** to compare algorithms implemented in different programming languages and run them without requiring unnecessary system privileges or installation of individual module dependencies. **Benchpress** is the first software of its kind for structure learning in many aspects, including scalability and reproducibility, and perhaps most importantly for the fact that it can directly incorporate existing software. This can potentially save researchers a large amount of unnecessary work and provide benchmarks that would never be implemented otherwise. Likewise, it could facilitate the implementation of comprehensive benchmarks for new algorithms, and the sharing of the results in a standardized format. In its current version **Benchpress** already implements 55 of the state-of-the-art learning algorithms, as well as several modules for generating data models and evaluating performance. As **Benchpress** is built in a completely modular form **Snakemake** allows for seamless scaling of computations over multiple cores, grids or servers without any extra additional effort. Furthermore, it is straightforward to integrate new modules into the workflow. Even though the **Benchpress** project focuses so far on structure learning for graphical models, we also see the potential in extending **Benchpress** to evaluate more general estimation procedures, also for other statistical models.

Acknowledgments

We would like to thank all the developers and researchers who made their software available open source. A special thanks to James Cussens and Mohamad Elmasri for their valuable feedback and their contributions towards expanding the package.

References

Anaconda Inc (2016). "**Anaconda** Software Distribution."

Andrews B, Ramsey J, Sanchez-Romero R, Camchong J, Kummerfeld E (2023). "Fast Scalable and Accurate Discovery of DAGs Using the Best Order Score Search and Grow-Shrink Trees." In *37th Conference on Neural Information Processing Systems (NeurIPS 2023).*

Atay-Kayis A, Massam H (2005). "A Monte Carlo Method for Computing the Marginal Likelihood in Nondecomposable Gaussian Graphical Models." *Biometrika*, **92**(2), 317–335. doi:10.1093/biomet/92.2.317.

Carvalho CM (2006). *Structure and Sparsity in High-Dimensional Multivariate Analysis.* Ph.D. thesis, Duke University.

Chickering DM (1995). "A Transformational Characterization of Equivalent Bayesian Network Structures." In *Proceedings of the Eleventh Conference on Uncertainty in Artificial Intelligence*, UAI'95, pp. 87–98. Morgan Kaufmann Publishers, San Francisco.

Chickering DM (2002). "Optimal Structure Identification with Greedy Search." *Journal of Machine Learning Research*, **3**(11), 507–554.

Chickering DM, Heckerman D, Meek C (2004). "Large-Sample Learning of Bayesian Networks Is NP-Hard." *Journal of Machine Learning Research*, **5**, 1287–1330. doi:10.1023/a:1022623210503.

Constantinou AC, Liu Y, Chobtham K, Guo Z, Kitson NK (2020). "The **Bayesys** Data and Bayesian Network Repository." *Queen Mary University of London*, pp. 2–2. doi:10.1007/s10618-022-00882-9.

Constantinou AC, Liu Y, Chobtham K, Guo Z, Kitson NK (2021). "Large-Scale Empirical Validation of Bayesian Network Structure Learning Algorithms with Noisy Data." *International Journal of Approximate Reasoning*, **131**, 151–188. doi:10.1016/j.ijar.2021.01.001.

Cowell RG, Dawid P, Lauritzen SL, Spiegelhalter DJ (2003). *Probabilistic Networks and Expert Systems: Exact Computational Methods for Bayesian Networks.* Information Science and Statistics. Springer-Verlag.

Cussens J (2011). "Bayesian Network Learning with Cutting Planes." In *Proceedings of the Twenty-Seventh Conference on Uncertainty in Artificial Intelligence*, UAI'11, pp. 153–160. AUAI Press, Arlington.

Cussens J (2020). "**GOBNILP**: Learning Bayesian Network Structure with Integer Programming." In *International Conference on Probabilistic Graphical Models*, pp. 605–608. PMLR.

Dawid AP, Lauritzen SL (1993). "Hyper Markov Laws in the Statistical Analysis of Decomposable Graphical Models." *The Annals of Statistics*, **21**(3), 1272–1317. doi:10.1214/aos/1176349260.

Diestel R (2005). *Graph Theory (Graduate Texts in Mathematics)*, volume 173. Springer-Verlag.

Duarte E, Solus L (2023). "A New Characterization of Discrete Decomposable Graphical Models." *Proceedings of the American Mathematical Society*, **151**, 1325–1338. doi:10.1090/proc/16212.

Edwards D (2012). *Introduction to Graphical Modelling*. Springer-Verlag.

Elmasri M (2017). "On Decomposable Random Graphs." *arXiv 1710.03283*, arXiv.org E-Print Archive. doi:10.48550/arXiv.1710.03283.

Elwert F (2013). "Graphical Causal Models." In *Handbook of Causal Analysis for Social Research*, pp. 245–273. Springer-Verlag.

Emerson JW, Green WA, Schloerke B, Crowley J, Cook D, Hofmann H, Wickham H (2013). "The Generalized Pairs Plot." *Journal of Computational and Graphical Statistics*, **22**(1), 79–91. doi:10.1080/10618600.2012.694762.

Friedman J, Hastie T, Tibshirani R (2008). "Sparse Inverse Covariance Estimation with the Graphical Lasso." *Biostatistics*, **9**(3), 432–441. doi:10.1093/biostatistics/kxm045.

Friedman N (2004). "Inferring Cellular Networks Using Probabilistic Graphical Models." *Science*, **303**(5659), 799–805. doi:10.1126/science.1094068.

Friedman N, Goldszmidt M, Heckerman D, Russell S (1997). "Where Is the Impact of Bayesian Networks in Learning." In *International Joint Conference on Artificial Intelligence*. Citeseer.

Friedman N, Koller D (2003). "Being Bayesian About Network Structure. A Bayesian Approach to Structure Discovery in Bayesian Networks." *Machine Learning*, **50**(1), 95–125. doi:10.1023/a:1020249912095.

Friedman N, Linial M, Nachman I, Pe'er D (2000). "Using Bayesian Networks to Analyze Expression Data." *Journal of Computational Biology*, **7**(3-4), 601–620. doi:10.1089/106652700750050961.

Geiger D, Heckerman D (1994). "Learning Gaussian Networks." In *Proceedings of the Tenth International Conference on Uncertainty in Artificial Intelligence*, pp. 235–243. Morgan Kaufmann Publishers.

Geiger D, Heckerman D (2002). "Parameter Priors for Directed Acyclic Graphical Models and the Characterization of Several Probability Distributions." *The Annals of Statistics*, **30**(5), 1412–1440. doi:10.1214/aos/1035844981.

Giudice E, Kuipers J, Moffa G (2023). "The Dual PC Algorithm and the Role of Gaussianity for Structure Learning of Bayesian Networks." *International Journal of Approximate Reasoning*, **161**, 108975. doi:10.1016/j.ijar.2023.108975.

Giudici P, Castelo R (2003). "Improving Markov Chain Monte Carlo Model Search for Data Mining." *Machine Learning*, **50**(1), 127–158. doi:10.1023/a:1020202028934.

Giudici P, Green PJ (1999). "Decomposable Graphical Gaussian Model Determination." *Biometrika*, **86**(4), 785–801. doi:10.1093/biomet/86.4.785.

Glymour C, Scheines R (1986). "Causal Modeling with the **TETRAD** Program." *Synthese*, **68**(1), 37–63. doi:10.1007/bf00413966.

Göbler K, Windisch T, Drton M, Pychynski T, Roth M, Sonntag S (2024). "**causalAssembly**: Generating Realistic Production Data for Benchmarking Causal Discovery." In F Locatello, V Didelez (eds.), *Proceedings of the Third Conference on Causal Learning and Reasoning*, volume 236 of *Proceedings of Machine Learning Research*, pp. 609–642. PMLR. URL https://proceedings.mlr.press/v236/gobler24a.html.

Green PJ, Thomas A (2013). "Sampling Decomposable Graphs Using a Markov Chain on Junction Trees." *Biometrika*, **100**(1), 91–110. doi:10.1093/biomet/ass052.

Hauser A, Bühlmann P (2012). "Characterization and Greedy Learning of Interventional Markov Equivalence Classes of Directed Acyclic Graphs." *The Journal of Machine Learning Research*, **13**(1), 2409–2464.

Hébert-Johnson Ú, Lokshtanov D, Vigoda E (2023). "Counting and Sampling Labeled Chordal Graphs in Polynomial Time." In IL Gørtz, M Farach-Colton, SJ Puglisi, G Herman (eds.), *31st Annual European Symposium on Algorithms (ESA 2023)*, volume 274 of *Leibniz International Proceedings in Informatics (LIPIcs)*, pp. 58:1–58:17. Schloss Dagstuhl – Leibniz-Zentrum für Informatik, Dagstuhl, Germany. doi:10.4230/lipics.esa.2023.58.

Heckerman D, Geiger D, Chickering DM (1995). "Learning Bayesian Networks: The Combination of Knowledge and Statistical Data." *Machine Learning*, **20**(3), 197–243. doi:10.1007/bf00994016.

Jennings D, Corcoran JN (2018). "A Birth and Death Process for Bayesian Network Structure Inference." *Probability in the Engineering and Informational Sciences*, **32**(4), 615–625. doi:10.1017/s0269964817000432.

Kalisch M, Mächler M, Colombo D, Maathuis MH, Bühlmann P (2012). "Causal Inference Using Graphical Models with the R Package **pcalg**." *Journal of Statistical Software*, **47**(11), 1–26. doi:10.18637/jss.v047.i11.

Kitson NK, Constantinou AC, Guo Z, Liu Y, Chobtham K (2023). "A Survey of Bayesian Network Structure Learning." *Artificial Intelligence Review*, pp. 1–94. doi:10.1007/s10462-022-10351-w.

Koller D, Friedman N (2009). *Probabilistic Graphical Models – Principles and Techniques.* MIT Press.

Koski T, Noble J (2012). "A Review of Bayesian Networks and Structure Learning." *Mathematica Applicanda*, **40**(1), 51–103. doi:10.14708/ma.v40i1.278.

Köster J, Rahmann S (2012). "**Snakemake** – A Scalable Bioinformatics Workflow Engine." *Bioinformatics*, **28**(19), 2520–2522. doi:10.1093/bioinformatics/bts480.

Kuipers J, Moffa G (2017). "Partition MCMC for Inference on Acyclic Digraphs." *Journal of the American Statistical Association*, **112**(517), 282–299. doi:10.1080/01621459.2015.1133426.

Kuipers J, Moffa G (2025). "The Interventional Bayesian Gaussian Equivalent Score for Bayesian Causal Inference with Unknown Soft Interventions." In B Huang, M Drton (eds.), *Proceedings of the Fourth Conference on Causal Learning and Reasoning*, volume 275 of *Proceedings of Machine Learning Research*, pp. 772–791.

Kuipers J, Moffa G, Heckerman D (2014). "Addendum on the Scoring of Gaussian Directed Acyclic Graphical Models." *The Annals of Statistics*, **42**(4), 1689–1691. doi:10.1214/14-aos1217.

Kuipers J, Moffa G, Kuipers E, Freeman D, Bebbington P (2019). "Links Between Psychotic and Neurotic Symptoms in the General Population: An Analysis of Longitudinal British National Survey Data Using Directed Acyclic Graphs." *Psychological Medicine*, **49**(3), 388–395. doi:10.1017/s0033291718000879.

Kuipers J, Suter P, Moffa G (2022). "Efficient Sampling and Structure Learning of Bayesian Networks." *Journal of Computational and Graphical Statistics*, **31**(3), 639–650. doi:10.1080/10618600.2021.2020127.

Kuipers J, Thurnherr T, Moffa G, Suter P, Behr J, Goosen R, Christofori G, Beerenwinkel N (2018). "Mutational Interactions Define Novel Cancer Subgroups." *Nature Communications*, **9**(1), 1–10. doi:10.1101/187260.

Kurtzer GM, Sochat V, Bauer MW (2017). "**Singularity**: Scientific Containers for Mobility of Compute." *PLOS One*, **12**(5), e0177459. doi:10.1371/journal.pone.0177459.

Lam WY, Andrews B, Ramsey J (2022). "Greedy Relaxations of the Sparsest Permutation Algorithm." In *Proceedings of the Thirty-Eighth Conference on Uncertainty in Artificial Intelligence*, volume 180 of *Proceedings of Machine Learning Research*, pp. 1052–1062. PMLR.

Lamprecht AL, Garcia L, Kuzak M, Martinez C, Arcila R, Martin Del Pico E, Dominguez Del Angel V, Van de Sandt S, Ison J, Martinez PA, McQuilton P, Valencia A, Harrow J, Psomopoulos F, Gelpi JL, Chue Hong N, Goble C, Capella-Gutierrez S (2020). "Towards FAIR Principles for Research Software." *Data Science*, **3**(1), 37–59. doi:10.3233/ds-190026.

Lauritzen SL (1996). *Graphical Models.* Oxford University Press.

Lenkoski A (2013). "A Direct Sampler for G-Wishart Variates." *Stat*, **2**(1), 119–128. doi:10.1002/sta4.23.

Madigan D, York J, Allard D (1995). "Bayesian Graphical Models for Discrete Data." *International Statistical Review*, **63**(2), 215–232. doi:10.2307/1403615.

Meek C (1997). *Graphical Models: Selecting Causal and Statistical Models*. Ph.D. thesis, Carnegie Mellon University.

Meinshausen N (2008). "A Note on the Lasso for Gaussian Graphical Model Selection." *Statistics and Probability Letters*, **78**(7), 880–884. doi:10.1016/j.spl.2007.09.014.

Merkel D (2014). "**Docker**: Lightweight Linux Containers for Consistent Development and Deployment." *Linux Journal*, **2014**(239), 2. doi:10.1007/978-1-4842-5826-2_3.

Moffa G, Catone G, Kuipers J, Kuipers E, Freeman D, Marwaha S, Lennox BR, Broome MR, Bebbington P (2017). "Using Directed Acyclic Graphs in Epidemiological Research in Psychosis: An Analysis of the Role of Bullying in Psychosis." *Schizophrenia Bulletin*, **43**(6), 1273–1279. doi:10.1093/schbul/sbx013.

Mohammadi R, Wit EC (2019). "**BDgraph**: An R Package for Bayesian Structure Learning in Graphical Models." *Journal of Statistical Software*, **89**(3), 1–30. doi:10.18637/jss.v089.i03.

Montagna F, Mastakouri AA, Eulig E, Noceti N, Rosasco L, Janzing D, Aragam B, Locatello F (2023). "Assumption Violations in Causal Discovery and the Robustness of Score Matching." In *Thirty-Seventh Conference on Neural Information Processing Systems*. URL https://openreview.net/forum?id=IyTArtpuCK.

Munafò MR, Nosek BA, Bishop DVM, Button KS, Chambers CD, Percie du Sert N, Simonsohn U, Wagenmakers EJ, Ware JJ, Ioannidis JPA (2017). "A Manifesto for Reproducible Science." *Nature Human Behaviour*, **1**(1), 0021. doi:10.1038/s41562-016-0021.

Ogarrio JM, Spirtes P, Ramsey J (2016). "A Hybrid Causal Search Algorithm for Latent Variable Models." In *Conference on Probabilistic Graphical Models*, pp. 368–379.

Olsson J, Pavlenko T, Rios FL (2019). "Bayesian Learning of Weakly Structural Markov Graph Laws Using Sequential Monte Carlo Methods." *Electronic Journal of Statistics*, **13**(2), 2865–2897. doi:10.1214/19-ejs1585.

Olsson J, Pavlenko T, Rios FL (2022). "Sequential Sampling of Junction Trees for Decomposable Graphs." *Statistics and Computing*, **32**(5), 1–18. doi:10.1007/s11222-022-10113-2.

Onisko A (2003). *Probabilistic Causal Models in Medicine: Application to Diagnosis in Liver Disorders*. Ph.D. thesis, Polish Academy of Science, Institute of Biocybernetics and Biomedical Engineering.

Pearl J (1995). "Causal Diagrams for Empirical Research." *Biometrika*, **82**(4), 669–688. doi:10.1093/biomet/82.4.669.

Pearl J (1997). *Probabilistic Reasoning in Intelligent Systems: Networks of Plausible Inference*. Representation and Reasoning Series. Morgan Kaufmann.

Pedregosa F, Varoquaux G, Gramfort A, Michel V, Thirion B, Grisel O, Blondel M, Prettenhofer P, Weiss R, Dubourg V, Vanderplas J, Passos A, Cournapeau D, Brucher M, Perrot M, Duchesnay E (2011). "**scikit-learn**: Machine Learning in Python." *Journal of Machine Learning Research*, **12**, 2825–2830.

Pezoa F, Reutter JL, Suarez F, Ugarte M, Vrgoč D (2016). "Foundations of JSON Schema." In *Proceedings of the 25th International Conference on World Wide Web*, pp. 263–273. International World Wide Web Conferences Steering Committee.

Ramsey JD (2021). "Improving Accuracy of Permutation DAG Search Using Best Order Score Search." *arXiv 2108.10141*, arXiv.org E-Print Archive. doi:10.48550/arXiv.2108.10141.

Ramsey JD, Malinsky D, Bui KV (2020). "**algcomparison**: Comparing the Performance of Graphical Structure Learning Algorithms with **TETRAD**." *Journal of Machine Learning Research*, **21**(238), 1–6.

Rantanen K, Hyttinen A, Järvisalo M (2017). "Learning Chordal Markov Networks via Branch and Bound." In I Guyon, UV Luxburg, S Bengio, H Wallach, R Fergus, S Vishwanathan, R Garnett (eds.), *Advances in Neural Information Processing Systems*, volume 30. Curran Associates.

Raskutti G, Uhler C (2018). "Learning Directed Acyclic Graph Models Based on Sparsest Permutations." *Stat*, **7**(1). doi:10.1002/sta4.183.

Reisach A, Seiler C, Weichwald S (2021). "Beware of the Simulated DAG! Causal Discovery Benchmarks May Be Easy to Game." In M Ranzato, A Beygelzimer, Y Dauphin, PS Liang, JW Vaughan (eds.), *Advances in Neural Information Processing Systems*, volume 34, pp. 27772–27784. Curran Associates.

Russell S, Norvig P (2002). *Artificial Intelligence: a Modern Approach*. Pearson.

Sachs K, Perez O, Pe'er D, Lauffenburger DA, Nolan GP (2005). "Causal Protein-Signaling Networks Derived from Multiparameter Single-Cell Data." *Science*, **308**(5721), 523–529. doi:10.1126/science.1105809.

Scanagatta M, Corani G, De Campos CP, Zaffalon M (2018). "Approximate Structure Learning for Large Bayesian Networks." *Machine Learning*, **107**(8-10), 1209–1227. doi:10.1007/s10994-018-5701-9.

Scanagatta M, De Campos CP, Corani G, Zaffalon M (2015). "Learning Bayesian Networks with Thousands of Variables." In *Advances in Neural Information Processing Systems*, pp. 1864–1872.

Scutari M (2010). "Learning Bayesian Networks with the **bnlearn** R Package." *Journal of Statistical Software*, **35**(3), 1–22. doi:10.18637/jss.v035.i03.

Scutari M, Graafland CE, Gutiérrez JM (2019a). "Who Learns Better Bayesian Network Structures: Accuracy and Speed of Structure Learning Algorithms." *International Journal of Approximate Reasoning*, **115**, 235–253. doi:10.1016/j.ijar.2019.10.003.

Scutari M, Vitolo C, Tucker A (2019b). "Learning Bayesian Networks from Big Data with Greedy Search: Computational Complexity and Efficient Implementation." *Statistics and Computing*, **29**(5), 1095–1108. doi:10.1007/s11222-019-09857-1.

Silander T, Kontkanen P, Myllymäki P (2007). "On Sensitivity of the MAP Bayesian Network Structure to the Equivalent Sample Size Parameter." In R Parr, L Van der Gaag (eds.), *Uncertainty in Artificial Intelligence*, pp. 360–367. AUAI Press.

Solus L, Wang Y, Uhler C (2021). "Consistency Guarantees for Greedy Permutation-Based Causal Inference Algorithms." *Biometrika*, **108**(4), 795–814. doi:10.1093/biomet/asaa104.

Spirtes P, Glymour CN (1991). "An Algorithm for Fast Recovery of Sparse Causal Graphs." *Social Science Computer Review*, **9**(1), 62–72. doi:10.1177/089443939100900106.

Studený M, Cussens J (2017). "Towards Using the Chordal Graph Polytope in Learning Decomposable Models." *International Journal of Approximate Reasoning*, **88**, 259–281. doi:10.1016/j.ijar.2017.06.001.

Suter P, Kuipers J, Moffa G, Beerenwinkel N (2023). "Bayesian Structure Learning and Sampling of Bayesian Networks with the R Package **BiDAG**." *Journal of Statistical Software*, **105**(9), 1–31. doi:10.18637/jss.v105.i09.

Teyssier M, Koller D (2005). "Ordering-Based Search: A Simple and Effective Algorithm for Learning Bayesian Networks." In *Proceedings of the Twenty-First Conference on Uncertainty in Artificial Intelligence*, UAI'05, pp. 584?–590. AUAI Press, Arlington.

Tsamardinos I, Aliferis CF, Statnikov AR, Statnikov E (2003). "Algorithms for Large Scale Markov Blanket Discovery." In *FLAIRS Conference*, volume 2, pp. 376–380.

Tsamardinos I, Brown LE, Aliferis CF (2006). "The Max-Min Hill-Climbing Bayesian Network Structure Learning Algorithm." *Machine Learning*, **65**(1), 31–78. doi:10.1007/s10994-006-6889-7.

Verma T, Pearl J (1991). *Equivalence and Synthesis of Causal Models*. UCLA, Computer Science Department.

Wang Y, Solus L, Yang K, Uhler C (2017). "Permutation-Based Causal Inference Algorithms with Interventions." In I Guyon, UV Luxburg, S Bengio, H Wallach, R Fergus, S Vishwanathan, R Garnett (eds.), *Advances in Neural Information Processing Systems*, volume 30. Curran Associates.

Waskom ML (2021). "**seaborn**: Statistical Data Visualization." *Journal of Open Source Software*, **6**(60), 3021. doi:10.21105/joss.03021.

Wickham H, Averick M, Bryan J, Chang W, McGowan LD, François R, Grolemund G, Hayes A, Henry L, Hester J, Kuhn M, Pedersen TL, Miller E, Bache SM, Müller K, Ooms J, Robinson D, Seidel DP, Spinu V, Takahashi K, Vaughan D, Wilke C, Woo K, Yutani H (2019). "Welcome to the **tidyverse**." *Journal of Open Source Software*, **4**(43), 1686. doi:10.21105/joss.01686.

Witten DM, Friedman JH, Simon N (2011). "New Insights and Faster Computations for the Graphical Lasso." *Journal of Computational and Graphical Statistics*, **20**(4), 892–900. doi:10.1198/jcgs.2011.11051a.

Wormald NC (1985). "Counting Labelled Chordal Graphs." *Graphs and Combinatorics*, **1**(1), 193–200. doi:10.1007/bf02582944.

Zhang K, Zhu S, Kalander M, Ng I, Ye J, Chen Z, Pan L (2021). "**gCastle**: A Python Toolbox for Causal Discovery." *arXiv 2111.15155*, arXiv.org E-Print Archive. doi:10.48550/arXiv.2111.15155.

Zheng X, Aragam B, Ravikumar PK, Xing EP (2018). "DAGs with NO TEARS: Continuous Optimization for Structure Learning." In *Advances in Neural Information Processing Systems*, pp. 9472–9483.

Zheng Y, Huang B, Chen W, Ramsey J, Gong M, Cai R, Shimizu S, Spirtes P, Zhang K (2024). "**causal-learn**: Causal Discovery in Python." *Journal of Machine Learning Research*, **25**(60), 1–8.

A. Graph metrics and data formats

A.1. Metrics

This section describes metrics for comparing graphs. We let $G = (V, E)$ and $G' = (V', E')$ denote the true and the estimated graph, respectively.

Structural Hamming distance

The *structural Hamming distance* (SHD) is one of the most commonly used metrics to compare graphs. It describes the number of changes, in terms of adding, removing or reversing edges or their directions, needed to transform E into E'.

True and false positive rates for mixed graphs

The following metric quantifies the difference between two *mixed graphs*, which may have a combination of directed and undirected edges. We let TP and FP be the true and also positive edge rates, but for directed edges, we include errors in their direction (wrong direction or directed where it should be undirected, or vice versa) as half a false positive (FP) and half a false negative (FN).

We assign to every edge $e \in E'$ the true positive score $TP(e) = 1$ if e is contained in E with the same orientation (e being undirected in both E and E' or e having the same direction in both E and E'), $TP(e) = 1/2$ if e is contained in E with a different orientation (or undirected when should be directed, or vice versa), otherwise $TP(e) = 0$.

The false positive score $FP(e)$ is defined analogously for every edge $e \in E'$. $FP(e) = 1$ if no orientation of e is contained in E and $FP(e) = 1/2$ if e is contained in E with a different orientation (or undirected when should be directed, or vice versa), otherwise $FP(e) = 0$.

The total true and false positive edges (TP and FP) are obtained as the sum of the individual edge scores, i.e.,

$$\mathrm{TP} := \sum_{e \in E'} TP(e), \quad \mathrm{FP} := \sum_{e \in E'} FP(e)$$

and the false negative edges (FN) are defined as

$$\mathrm{FN} := \mathrm{P} - \mathrm{TP},$$

where $\mathrm{P} := |E|$ denotes the total number of edges in G. Note that TP, FP, and FN reduce to the ordinary true and false positives and false negatives, respectively, when all edges are undirected in both G and G'.

We often consider the scaled true and false positive rates FP/P and TP/P, since the SHD, also for mixed graphs, can easily be determined in a ROC-type figure as the scaled *Manhattan distance* between the points (0,1) and (TP/P, FP/P), i.e.,

$$\mathrm{SHD}/\mathrm{P} = 1 - \mathrm{TP}/\mathrm{P} + \mathrm{FP}/\mathrm{P}.$$

F score

The *precision* (PR) and *recall* (RE) metrics are defined as

$$\mathrm{PR} := \frac{\mathrm{TP}}{\mathrm{TP}+\mathrm{FP}}, \quad \mathrm{RE} := \frac{\mathrm{TP}}{\mathrm{TP}+\mathrm{FN}}.$$

For any $\beta \geq 0$ the F_β score is defined as

$$F_\beta := (1+\beta^2)\frac{\mathrm{PR}\cdot\mathrm{RE}}{\beta^2\mathrm{PR}+\mathrm{RE}}.$$

Benchpress uses $\beta = 1$ as default which simplifies to

$$F_1 = \frac{\mathrm{PR}\cdot\mathrm{RE}}{\mathrm{PR}+\mathrm{RE}} = \frac{2\mathrm{TP}}{2\mathrm{TP}+\mathrm{FP}+\mathrm{FN}}.$$

A.2. Data formats

Throughout this section for simplicity we consider a four dimensional graphical model where the nodes are labeled as *a,b,c* and *d*.

Data set

Observations should be stored as row vectors in a matrix, where the columns are separated by commas. The first row should contain the labels of the variables and if the data is categorical, the second row should contain the cardinality (number of levels) of each variable.

Below is a formatting example of two samples of a categorical distribution where the cardinalities are 2,3,2, and 2.

```
a,b,c,d
2,3,2,2
1,2,0,1
0,1,1,1
```

An example showing of two samples from continuous distribution is shown below.

```
a,b,c,d
0.2,2.3,5.3,0.5
3.2,1.5,2.5,1.2
```

Adjacency matrix

A graph $G = (E, V)$ is represented by its adjacency matrix M, where $M_{ij} = 1$ if $(i,j) \in E$ and $M_{ij} = 0$ if $(i,j) \notin E$. An undirected graph is represented by a symmetric matrix.

Below is an example undirected graph $G = (V, E)$, where $E = \{(a,b),(a,c),(c,d)\}$ are interpreted as un-ordered pairs (un-directed edges).

```
a,b,c,d
0,1,1,0
1,0,0,0
1,0,0,1
0,0,1,0
```

If G is directed the adjacency matrix is asymmetric as below.

```
a,b,c,d
0,1,1,0
0,0,0,0
0,0,0,1
0,0,0,0
```

MCMC trajectory

When the output of the algorithm is a Markov chain of graphs, we store the output in a compact form by tracking only the changes when moves are accepted, along with the corresponding time index and the score of the resulting graph after acceptance (not the score difference).

Additionally, in the first two rows the labels of the variables, which should be read from the data matrix, are recorded. Specifically, the first row (index -2) contains edges from the first variable to each of the rest in the `added` column, where a dash (`-`) symbolizes an undirected edge, and a right arrow (`->`) a directed edge. The `score` column is set to 0 and `removed` is set to `[]`. The second row (index -1) has the same edges in the `removed` column, while the `score` column is set to 0 and `added` is set to `[]`. The third row (index 0) contains all the vertices in the starting graph along with its score in the `score` column and `[]` in the `removed` column.

Below is an example of a trajectory of undirected graphs $G_0, G_1, \ldots, G_{89}$, where $E_i = \{(b,c),(a,d)\}$ for $i = 0,\ldots,33$, $E_i = \{(a,d)\}$ for $i = 34,\ldots,88$ and $E_i = \{(c,d),(a,d)\}$ for $i = 89$.

```
index,score,added,removed
-2,0.0,[a-b;a-c;a-d],[]
-1,0.0,[],[a-b;a-c;a-d]
0,-2325.52,[b-c;a-d],[]
34,-2311.94,[],[b-c]
89,-2310.81,[c-d],[]
```

B. Benchpress modules

B.1. Graph modules

Random graph (`pcalg_randdag`)

The `pcalg_randdag` module samples random undirected graphs and DAGs using the *randDAG* function from the **pcalg** package (Kalisch *et al.* 2012), with the additional option of restricting the maximal number of parents per node.

Fixed graph (`fixed_graph`)

A fixed graph is represented as an adjacency matrix and should be formatted as specified in Appendix A. The file should be stored with the `.csv` extension in the directory `resources/adjmat/myadjmats/`.

B.2. Parameters modules

Random binary Bayesian network (`bin_bn`)

This module samples the conditional probability tables of a binary Bayesian network (only binary variables). For each variable Y_i and parent configuration $\mathrm{pa}(y_i)$

$$\Pr(Y_i = 0 \mid \mathrm{pa}(y_i)) \sim \mathrm{Unif}([a, b]),$$

where $(a, b) \in [0, 1]^2, a < b$ and $\mathrm{Unif}(c)$ denotes the uniform distribution on the range c.

Random linear Gaussian Bayesian network (`sem_params`)

This module samples the weight matrix W of a Gaussian linear structural equation model (SEM) of the form

$$Y_i = \sum_{j:Y_j \in \mathrm{pa}(Y_i)} W_{ij} Y_j + Z_i, \tag{1}$$

where $Z_i \sim \mathcal{N}(\mu, \sigma^2)$ and elements of W are distributed as

$$W_{ij} \sim \begin{cases} \mathrm{Unif}([a, b])\mathrm{Unif}(\{-1, 1\}) & \text{if } (i, j) \in E \\ 0 & \text{otherwise.} \end{cases} \tag{2}$$

Fixed parameters (`fixed_params`)

Two types of fixed parameters are currently supported and described below.

- ‘`bn.fit`’ *object*: A Bayesian network object in the R-package **bnlearn** (Scutari 2010) is an instance of the ‘`bn.fit`’ class and contains both the DAG and corresponding parameters. Motivated by the modular design of **Benchpress**, a ‘`bn.fit`’ object may be used to specify only the parameters of a Bayesian network, by storing it in `.rds` format in `resources/parameters/myparams/bn.fit_networks/`. The adjacency matrix of the DAG should be stored in the folder for `fixed_graphs` and `graph_id` should be set to the filename.

- *SEM parameters matrix*: A matrix defining the weights W in a SEM as defined in (1) can be stored in `resources/parameters/myparams/sem_params/` with the `.csv` extension, formatted as the adjacency matrix specified in Appendix A.

Gaussian graph intra-class model (`trilearn_intraclass`)

This module specifies the covariance matrix Σ of a zero-mean Gaussian graphical model by the solution of the following matrix completion problem

$$\begin{aligned} \Sigma_{ij} &= \begin{cases} \sigma^2, & \text{if } i = j \\ \rho\sigma^2, & \text{if } (i,j) \in E \end{cases} \\ (\Sigma^{-1})_{ij} &= 0 \qquad\qquad \text{if } (i,j) \notin E, \end{aligned}$$

where $\sigma^2 > 0$ and $\rho \in [0,1]$ denote the variance and correlation coefficient, respectively.

Hyper Dirichlet (`trilearn_hyper-dir`)

This module samples the parameters of a categorical decomposable model from the *hyper Dirichlet* distribution (Dawid and Lauritzen 1993), with a specified concentration parameter and number of levels per variable.

Inverse G-Wishart (`bdgraph_rgwish`)

This modules samples the precision matrix of a Gaussian graphical model from the *G-Wishart* distribution (Dawid and Lauritzen 1993; Atay-Kayis and Massam 2005; Lenkoski 2013) using the `rgwish` function from the **BDgraph** package (Mohammadi and Wit 2019). The clique-wise scale matrices are fixed to the identity matrix while the degrees of freedom and a threshold value for the convergence of the sampling algorithm are specified by the user.

B.3. Data modules

Fixed data sets (`fixed_data`)

The are two ways of providing fixed data sets. The first option is to place data files directly in the directory `resources/data/mydatasets/` with the `.csv` extension, formatted according to Appendix A. The second option is to place the files in a sub directory of `resources/data/mydatasets/`. In the latter case, the `data_id` field in the `benchmarks_setup` section should be the name of the directory and all the files in it will be considered for evaluation.

IID samples (`iid`)

An object of the `iid` module will draw a specified (`n`) number of independent samples from a specified model. Continuous data may be standardized by setting `standardized` to `true`. See Reisach, Seiler, and Weichwald (2021) for a discussion about standardizing data in a structure learning context.

B.4. Structure learning algorithms

This section contains a short summary of the structure learning modules that are used in the simulation study of Section 5.

Algorithm	Graph	Package	Module
ANM	DAG	**gCastle**	`gcastle_anm`
ASOBS	DAG	**r.blip**	`rblip_asobs`
BDgraph	UG	**BDgraph**	`bdgraph`
BOSS	CPDAG	**causal-cmd**	`tetrad_boss`
Chordal graph samplers	DG		`athomas_jtsamplers`
CORL	DAG	**gCastle**	`gcastle_corl`
Corrmat thresh	UG	**Benchpress**	`corr_thresh`
Direct LINGAM	DAG	**gCastle**	`gcastle_direct_lingam`
Dual PC	CPDAG	**dualPC**	`dualpc`
FAS	DAG	**causal-cmd**	`tetrad_fas`
FASK	DAG	**causal-cmd**	`tetrad_fask`
Fast IAMB	DAG	**bnlearn**	`bnlearn_fastiamb`
FGES	CPDAG	**causal-cmd**	`tetrad_fges`
FOFC	DAG	**causal-cmd**	`tetrad_fofc`
FTFC	DAG	**causal-cmd**	`tetrad_ftfc`
GAE	DAG	**gCastle**	`gcastle_gae`
GIES	CPDAG	**pcalg**	`pcalg_gies`
GOBNILP	DAG	**GOBNILP**	`gobnilp`
GOLEM	DAG	**gCastle**	`gcastle_golem`
GraNDAG	DAG	**gCastle**	`gcastle_grandag`
Graphical Lasso	UG	**scikit-learn**	`sklearn_glasso`
GRaSP	CPDAG	**causal-learn**	`causallearn_grasp`
GRaSP	CPDAG	**causal-cmd**	`tetrad_grasp`
Grow-shrink	DAG	**bnlearn**	`bnlearn_gs`
GrUES	UG	**gues**	`grues`
GSP	DAG	**CausalDAG**	`causaldag_gsp`
H2PC	DAG	**bnlearn**	`bnlearn_h2pc`
HC	DAG	**bnlearn**	`bnlearn_hc`
HPC	DAG	**bnlearn**	`bnlearn_hpc`
IAMB	DAG	**bnlearn**	`bnlearn_iamb`
IAMB-FDR	DAG	**bnlearn**	`bnlearn_iambfdr`
ICALiNGAM	DAG	**gCastle**	`gcastle_ica_lingam`
INTER-IAMB	DAG	**bnlearn**	`bnlearn_interiamb`
Iterative search	DAG	**BiDAG**	`bidag_itsearch`
LINGAM	DAG	**causal-cmd**	`tetrad_lingam`
MCSL	DAG	**gCastle**	`gcastle_mcsl`
MMHC	DAG	**bnlearn**	`bnlearn_mmhc`
MMPC	DAG	**bnlearn**	`bnlearn_mmpc`
NO TEARS	DAG	**gCastle**	`gcastle_notears`
NO TEARS low rank	DAG	**gCastle**	`gcastle_notears_low_rank`
NO TEARS non-linear	DAG	**gCastle**	`gcastle_notears_nonlinear`
Order MCMC	DAG	**BiDAG**	`bidag_order_mcmc`
Parallel DG	DG	**parallelDG**	`paralleldg`
Particle Gibbs	DG	**trilearn**	`trilearn_pgibbs`
Partition MCMC	DAG	**BiDAG**	`bidag_partition_mcmc`
PC	CPDAG	**bnlearn**	`bnlearn_pcstable`
PC	DAG	**gCastle**	`gcastle_pc`
PC	CPDAG	**pcalg**	`pcalg_pc`
PC-ALL	DAG	**causal-cmd**	`tetrad_pc-all`
Precmat thresh	UG	**Benchpress**	`prec_thresh`
Psi-leaner	UG	**equSA**	`equsa_psilearner`
RL	DAG	**gCastle**	`gcastle_rl`
RSMAX2	DAG	**bnlearn**	`bnlearn_rsmax2`
S-I HITON-PC	DAG	**bnlearn**	`bnlearn_sihitonpc`
Tabu	DAG	**bnlearn**	`bnlearn_tabu`

Table 6: Currently available structure learning modules.

Peter and Clark (`pcalg_pc`)

The *Peter and Clark* (PC) algorithm (Spirtes and Glymour 1991), is a constraint based method consisting of two main steps. The first step is called the *adjacency search* and amounts to finding the undirected skeleton of the DAG through conditional independence tests. The second step consists of estimating a CPDAG from the skeleton and the previous tests.

Dual PC (`dualpc`)

The *dual PC* algorithm (Giudice, Kuipers, and Moffa 2023) is an alternative scheme to carry out the conditional independence tests within the PC algorithm for Gaussian data, by leveraging the inverse relationship between covariance and precision matrices. The algorithm exploits block matrix inversions on the covariance and precision matrices to simultaneously perform tests on partial correlations of complementary (or dual) conditioning sets. Simulation studies indicate that the dual PC algorithm outperforms the classic PC algorithm both in terms of run time and in recovering the underlying network structure.

Hill climbing (`bnlearn_hc`)

Hill climbing (HC) is a score-based algorithm that starts with a DAG with no edges and adds, deletes, or reverses edges in a greedy manner until an optimum is reached (Russell and Norvig 2002; Scutari, Vitolo, and Tucker 2019b).

Tabu (`bnlearn_tabu`)

Tabu is a less greedy version of the HC algorithm allowing for non-optimal moves that might be beneficial from a global perspective to avoid local maxima (Russell and Norvig 2002; Scutari *et al.* 2019b).

Best order score search (`tetrad_boss`)

Best order score search (BOSS) (Ramsey 2021; Andrews, Ramsey, Sanchez-Romero, Camchong, and Kummerfeld 2023) is a permutation-based algorithm stemming from the *ordering search* (OS) of Teyssier and Koller (2005) and the *sparsest permutation* (SP) algorithm of Raskutti and Uhler (2018) as in the *greedy sparsest permutation* (GSP) algorithm of Solus, Wang, and Uhler (2021). BOSS gives results as accurate as SP but for much larger and denser graphs. It is more accurate for two reasons: (a) It assumes the so-called *brute faithfulness* assumption, which is weaker than faithfulness, and (b) it uses a different traversal of permutations than the depth-first traversal used by GSP, obtained by taking each variable in turn and moving it to the position in the permutation that optimizes the model score.

Fast greedy equivalent search (`tetrad_fges`)

Fast greedy equivalent search (FGES) is a score based method based on the the greedy equivalence search (GES) of Meek (1997). This algorithm operates on the space of CPDAG's (Chickering 2002). Its complexity is polynomial in the number of nodes. The FGES is asymptotically correct under the assumption that there are no unmeasured confounders (Ogarrio, Spirtes, and Ramsey 2016), a condition required for most algorithms with convergence guarantees.

Greedy relaxations of the sparsest permutation algorithm (`tetrad_grasp`)

This is a method that exploits permutation reasoning to search for directed acyclic causal models, like the OS algorithm of Teyssier and Koller (2005) and GSP of Solus *et al.* (2021). The algorithm extends these methods by a permutation-based operation called *tuck*, and develops a class of algorithms, namely *greedy relaxations of the sparsest permutation* (GRaSP) (Lam, Andrews, and Ramsey 2022), that are computationally efficient and pointwise consistent under increasingly weaker assumptions than faithfulness.

Order Markov chain Monte Carlo (`bidag_order_mcmc`)

This technique relies on a Bayesian perspective on structure learning and uses the posterior probability of graphs as a score. To overcome the limitation of simple structure-based MCMC schemes, Friedman and Koller (2003) turned to a score defined as the sum of the posterior scores of all DAG which are consistent with a given topological ordering of the nodes. One can then run a Metropolis-Hasting algorithm to sample from the distribution induced by the order score, and later draw a DAG consistent with the order. This strategy substantially improves convergence with respect to earlier structure MCMC scheme, though it unfortunately produces a biased sample on the space of DAGs. The bias can be removed by operating on the space of ordered partitions instead (Kuipers and Moffa 2017). The implementation considered in **Benchpress** is a hybrid version with the sampling performed on a restricted search space initialized with constraint-based testing and improved with a score-based search (Kuipers *et al.* 2022).

Max-min hill-climbing (`bnlearn_mmhc`)

Max-min hill-climbing (MMHC) is a hybrid method which first estimates the skeleton of a DAG using an algorithm called *max-min parents and children* and then performs a greedy hill-climbing search to orient the edges with respect to a Bayesian score (Tsamardinos *et al.* 2006). It is a popular approach used as standard benchmark and also well suited for high-dimensional domains.

Globally optimal Bayesian network learning using integer linear programming (`gobnilp`)

A score based method using integer linear programming (ILP) for learning an optimal DAG for a Bayesian network with limit on the maximal number of parents for each node (Cussens 2011). It is a two-stage approach where candidate parent sets for each node are discovered in the first phase and the optimal sets are determined in a second phase.

Acyclic selection ordering-based search (`rblip_asobs`)

A score-based two-phase algorithm where the first phase aims to identify the possible parent sets, Scanagatta *et al.* (2015); Scanagatta, Corani, De Campos, and Zaffalon (2018). The second phase performs an optimization on a modification of the space of node orders introduced in Teyssier and Koller (2005), allowing edges from nodes of higher to lower order, provided that no cycles are introduced.

Iterative search (`bidag_itsearch`)

This is a hybrid score-based optimization technique based on MCMC schemes (Suter *et al.* 2023; Kuipers *et al.* 2022). The algorithm starts from a skeleton obtained through a fast method (e.g., a constraint based method, or GES). Then it performs score and search on the DAGs belonging to the space defined by the starting skeleton. To correct for edges which may be missed, the search space is iteratively expanded to include one additional parent for each variable from outside the current search space. The score and search phase relies on an MCMC scheme producing a chain of DAGs from their posterior probability given the data.

No tears (`gcastle_notears`)

This score-based method recasts the combinatorial problem of estimating a DAG into a purely continuous non-convex optimization problem over real matrices with a smooth constraint to ensure acyclicity (Zheng, Aragam, Ravikumar, and Xing 2018).

B.5. Evaluation modules

Standard benchmarking metrics (`benchmarks`)

The relative performance of algorithms may differ depending on the evaluation metric, and no single metric is generally preferred. Therefore, to get an overall picture of the performance of an algorithm, the `benchmarks` module supports different metrics. The `benchmarks` module provides standard benchmarking metrics in terms of computational time, F_1, FN, TP, and FP, etc. (see Appendix A.1 for definitions).

In addition to the CSV summaries, **Benchpress** also provides visual summarizes in terms of, e.g., box-plots and receiver operating characteristics (ROC) type curves using the R-package **ggplot2** (Wickham *et al.* 2019) (see, e.g., Figure 2a and Figure 8). Since the true graphs are needed for evaluations, this module works for data scenarios (II–V).

Pair-wise plots of the data (`ggally_ggpairs`)

The `ggally_ggpairs` module produces pair-wise plots of the data using the `ggpairs` function (Emerson *et al.* 2013) from the R-package **GGally** (see Figure 3 for an example).

Plot estimated graphs (`graph_plots`)

The `graph_plots` module plots and saves the estimated graphs and adjacency matrices (see Figure 5a and 5b for examples). If the true graph is available it also compares the true to the estimated graphs using `graphviz.compare` function from the **bnlearn** package (see Figure 6 for an example).

Plot true graphs (`graph_true_plots`)

The `graph_true_plots` module plots the true underlying graphs and corresponding adjacency matrices.

Statistics for true graphs (`graph_true_stats`)

The `graph_true_stats` module computes properties of the true underlying graphs and stored in a CSV file and plotted. See Figure 2b for an example plot from this module.

MCMC mean graphs (`mcmc_heatmaps`)

For Bayesian inference it is customary to use MCMC methods to simulate a Markov chain of graphs $\{G^l\}_{l=0}^{\infty}$ having the graph posterior as stationary distribution. Suppose we have a realization of length M of such chain, then the posterior probability of an edge e is estimated by $\frac{1}{M+1-b}\sum_{l=b}^{M}\mathbf{1}_e(e^l)$, where the first samples up to b are disregarded as a burn-in period. The `mcmc_heatmaps` module has a list of objects, where each object has an `id` field for the algorithm object `id` and a burn-in field (`burn_in`) for specifying the burn-in period.

MCMC trajectory plots (`mcmc_traj_plots`)

The `mcmc_traj_plots` module plots the value of a given functional for the graphs in the MCMC trajectory. The currently supported functionals are the number of edges for the graphs (`size`) and the score (`score`). The `mcmc_traj_plots` module has a list of objects, where each object has an `id` field for the algorithm object `id`, a burn-in field (`burn_in`) and a field specifying the functional to be considered (`functional`). Since the trajectories may be very long, the user may choose to thin out the trajectory by only considering every graph at a given interval length specified by the `thinning` field.

MCMC auto-correlation plots (`mcmc_autocorr_plots`)

The `mcmc_autocorr_plots` module plots the auto-correlation of a functional of the graphs in a MCMC trajectory. Similar to the `mcmc_traj_plots` module, the `mcmc_autocorr_plots` module has a list of objects, where each object has an `id`, `burn_in`, `thinning`, and a `functional` field. The maximum number of lags after thinning, is specified by the `lags` field.

Affiliation:

Felix L. Rios, Giusi Moffa
University of Basel
Department of Mathematics and Computer Science
Spiegelgasse 1, 4051 Basel, Switzerland
E-mail: felix.leopoldo.rios@gmail.com, giusi.moffa@unibas.ch

Jack Kuipers
ETH Zürich
Department of Biosystems Science and Engineering
Mattenstrasse 26, 4058 Basel, Switzerland
E-mail: jack.kuipers@bsse.ethz.ch

Journal of Statistical Software https://www.jstatsoft.org/
published by the Foundation for Open Access Statistics https://www.foastat.org/
October 2025, Volume 114, Issue 12 *Submitted:* 2022-05-27
doi:10.18637/jss.v114.i12 *Accepted:* 2024-07-01